Generator Excitation Controller

Major Project Report

Submitted in Partial Fulfillment of the Requirements for the
Degree of

Master of Technology
in
Electrical Engineering
(Electrical Power Systems)

By

Sharma Vimal R.
15MEEE23

DEPARTMENT OF ELECTRICAL ENGINEERING
INSTITUTE OF TECHNOLOGY
NIRMA UNIVERSITY
AHMEDABAD-382481
May-2017

Certificate

This is to certify that the Major Project Report entitled **Generator Excitation Controller** submitted by **Mr. Sharma Vimal R. (15MEEE23)** towards the partial fulfillment of the requirements for Semester-IV of Master of Technology (Electrical Engineering) in the field of Electrical Power Systems of Nirma University is the record of work carried out by him under our supervision and guidance. The work submitted has in our opinion reached a level required for being accepted for examination. The results embodied in this major project work to the best of our knowledge have not been submitted to any other University or Institution for award of any degree or diploma.

Date:

Prof. Chanakya B. Bhatt
Assistant Professor,
Electrical Engineering,
Institute of Technology,
Nirma University

Mr. Vinod Patel
Industry Guide
DGM, Research and Development,
Amtech Electronics India Limited,
Gandhinagar (Gujarat)

Prof. P.N. Tekwani
Head of Department,
Electrical Engineering,
Institute of Technology,
Nirma University
Ahmedabad

Prof. Alka Mahajan
Director
Institute of Technology
Nirma University
Ahmedabad

Undertaking for Originality of the Work

I, **Sharma Vimal R., Roll No. 15MEEE23**, give undertaking that the Major Project entitled **Generator Excitation Controller** submitted by me, towards the partial fulfillment of the requirements for the degree of Master of Technology in **Electrical Power Systems, Electrical Engineering** of Nirma University, Ahmedabad, is the original work carried out by me and I give assurance that no attempt of plagiarism has been made. I understand that in the event of any similarity found subsequently with any published work or any dissertation work elsewhere; it will result in severe disciplinary action.

.....
Signature of Student

Date: .....

Place: .....

Endorsed By:

.....
(Mr.Vinod Patel)
(Signature of Industry Guide)

.....
(Prof. Chanakya B. Bhatt)
(Signature of Institute Guide)

Acknowledgement

I would like to express my immense gratitude to my mentors Mr.Vinod Patel, DGM(Research and Development), Amtech Electronics India Limited and Prof. Chanakya B. Bhatt, Department of Electrical Engineering, Nirma University, Ahmedabad for their valuable guidance and continual encouragement throughout my project work. Their constant support and interest equipped me with a great understanding of different aspects.

A special thanks to Prof. P. N. Tekwani(Head of Department) and Prof. Santosh C. Vora(PG coordinator, EPS), of Department of Electrical Engineering, Institute of Technology, Nirma University, Ahmedabad for allowing us to carry out industrial training at this place.

Most importantly deepest appreciation and thanks to Almighty and my family for their unending love, affection and personal sacrifices during the whole tenure of my study.

Abstract

Traditionally, the generator excitation systems were meant only to provide field current to the field winding of the synchronous generators. Hence initially, dc generator based excitation controllers were used. With the advent of fast acting semiconductor switches, static excitation systems were developed that were having very fast response time. With the development of static excitation systems, Automatic Voltage Regulators (AVR) and Power System Stabilizers (PSS) were also developed to improve the transient stability and small signal stability respectively. The aim of this project is to design a generator excitation controller that have faster response and can improve the transient stability as well as small signal stability with reduced cost and increased robustness. Currently the AVR and PSS function separately and in many cases the hardware is also different. Hence the project aims at designing the controller that can perform the function of both the AVR and PSS. The different control strategies proposed by authors are compared and analyzed on Single Machine Infinite Bus and according to the excitation response of algorithms, the response of exciters are also obtained.

Contents

Certificate ii

Undertaking for Originality of the Work iii

Acknowledgement iv

Abstract v

Contents vii

List of Figures ix

Abbreviation and Nomenclature x

1 Introduction 1
1.1 Types of Excitation Systems 1

2 Literature Survey 3

3 Simulations of Static Excitation System and H-P constants 7
3.1 Thyristor Excitation System 7
3.2 Diode Full bridge rectifier with Buck converter excitation system . . . 8
3.3 Heffron-Phillips constants model 10

4 Excitation system response in a Radial System 12

5 Excitation System Response in SMIB system 19

6 Implementation of IDA-PBC control 25

7 Reduction of Signal requirement 31
7.1 State Estimation of Active and Reactive Powers 32
7.2 Load Angle δ Estimation 35
7.3 Rotor Speed Estimation 37

8 Implementation of AVR and PSS **41**
8.1 Implementation of Automatic Voltage Regulators (AVR) only 41
8.2 Implementation of Power System Stabilizers (PSS) 42
8.3 Flowchart 43

9 Hardware Implementation **46**
9.1 Generation of firing pulses and excitation output voltage signal (E_{fd}) 46
9.1.1 Generation of E_{fd} 46
9.1.2 Generation of firing pulses 47
9.2 Response of fully controlled thyristor bridge rectifier 52

10 Conclusion and Future Scope **54**
10.1 Conclusion 54
10.2 Future Scope 54

11 References **55**

List of Figures

3.1 Thyristor Full Bridge Rectifier 7
3.2 Output Voltage and Input Current for Thyristor Rectifier. [X-axis: 0.02 s/div.; Y-axis: Plot1: 50 V/div., Plot2: 20 A/div.] 8
3.3 Diode Full Bridge Rectifier with Buck Converter 8
3.4 Pulses for IGBT Control. [X-axis: 0.01 s/div.; Y-axis: Plot1: 1 V/div., Plot2: 0.2 pu/div.] 9
3.5 Output of Diode Full bridge Type Excitation System. [X-axis: 0.02 s/div.; Y-axis: Plot1: 50 V/div., Plot2: 10 A/div.] 10
3.6 Heffron Phillips Constants Model 11

4.1 Single Machine Infinite Bus 13
4.2 Voltage, Current, Rotor Mechanical Angle, Fault Current. [X-axis: 0.1 s/div.; Y-axis: Plot1: 0.5 pu/div., Plot2: 50 kA/div., Plot3: 10 rad/div., Plot4: 2 kA/div.] 13
4.3 V_d, V_q, Terminal Voltage(pu) and Load Angle(degree) 14
4.4 V_d, V_q, Terminal Voltage(pu) and Load Angle(degree) 14
4.5 MATLAB Excitation System Response under Radial Condition . . . 15
4.6 Feedback Linearization AVR 15
4.7 Voltage, Current, Rotor mechanical angle, Fault current [X-axis: 0.1 s/div.; Y-axis: Plot1: 0.5 pu/div., Plot2: 50 kA/div., Plot3: 10 rad/div., Plot4: 2 kA/div.] 16
4.8 V_d, V_q, Terminal Voltage(pu) and Load Angle(degree) 17
4.9 V_d, V_q, Terminal Voltage(pu) and Load Angle(degree) 17
4.10 Excitation Voltage Response of FBLAVR under Radial Condition . . 18
4.11 Field Current FBLAVR 18

5.1 Voltage, Current, Rotor mechanical angle, Fault current 20
5.2 V_d, V_q, Terminal Voltage(pu) and Load Angle(degree) 20
5.3 V_d, V_q, Terminal Voltage(pu) and Load Angle(degree) 21
5.4 MATLAB Excitation System Response in SMIB 21
5.5 Voltage, Current, Rotor Mechanical angle, Fault Current 22
5.6 V_d, V_q, Terminal Voltage(pu) and Load Angle(degree) 22
5.7 V_d, V_q, Terminal Voltage(pu) and Load Angle(degree) 23

5.8 Excitation Voltage Response of FBLAVR under Radial Condition . . 23
5.9 Field Current FBLAVR 24

6.1 Excitation response of AVR. [X-axis: 0.5 s/div.; Y-axis: 2 pu/div.] . . 26
6.2 Excitation Response for IDA-PBC case. [X-axis: 0.5 s/div.; Y-axis: 0.1 pu/div.] 27
6.3 Active and Reactive Power for AVR case. [X-axis: 0.5 s/div.; Y-axis: 0.002 pu/div.] 27
6.4 Active and Reactive Power with IDA-PBC. [X-axis: 0.5 s/div.; Y-axis: 0.002 pu/div.] 28
6.5 Terminal Voltage and Rotor Speed with AVR. [X-axis: 0.5 s/div.; Y-axis: Plot1: 0.2 pu/div., Plot2: 0.01 pu/div.] 28
6.6 Terminal Voltage and Rotor speed with IDA-PBC. [X-axis: 0.5 s/div.; Y-axis: Plot1: 0.2 pu/div., Plot2: 0.01 pu/div.] 29
6.7 Load Angle with AVR. [X-axis: 0.5 s/div.; Y-axis: 5 degrees/div.] . . 29
6.8 Load Angle Power with IDA-PBC. [X-axis: 0.5 s/div.; Y-axis: 5 degrees/div.] 30

7.1 Flowchart for rotor oscillation frequency 39
7.2 Estimated and Measured variables. [X-axis: 0.5 s/div.; Y-axis: Plot1: 50 degree/div., Plot2: 0.5 pu/div., Plot3: 0.5 pu/div.] 40
7.3 Rotor and Power oscillations. [X-axis: 0.5 s/div.; Y-axis: Plot1: 0.005 rad/div., Plot2: 0.01 pu/div., Plot3: 0.01 pu/div., Plot4: 0.5 pu/div.] 40

8.1 Flowchart for AVR+PSS implementation 45

9.1 MATLAB Simulation for E_{fd} and Firing Pulses 47
9.2 Simulation Result for E_{fd} and Firing Pulses. [X-axis: 0.1 s/div.; Y-axis: Plot1: 0.01 pu/div, Plot2: 0.2 pu/div.] 48
9.3 DSpace Simulation 49
9.4 Response of changing V_t on firing pulses 50
9.5 Firing Pulses for Thyristor Switches 50
9.6 Firing Pulses for T_1 and T_4 for different V_t and V_{ref} 51
9.7 Block Diagram of Hardware Implementation 52
9.8 Thyristor Excitation Response for varying V_{dc} 53

Abbreviation and Nomenclature

SMIB	Single Machine Infinite Bus
FBLAVR	Feedback Linearization Automatic Voltage Regulator
AVR	Automatic Voltage Regulator
PSS	Power System Stabilizer
IDA-PBC	Interconnection and Damping Assignment Passivity Based Control
DECS	Digital Excitation Control System
V_d	D-axis Component of Terminal Voltage
V_q	Q-axis Component of Terminal Voltage
V_{ab}, V_{bc}, V_{ca}	Three phase to phase voltages
I_a, I_b, I_c	Three line currents
ω	Mechanical Speed rad/s
δ	Load Angle
P	Active Power
Q	Reactive power
S	Apparent power
R	Armature resistance of synchronous generator
X_q	Quadrature axis reactance for cylindrical type synchronous generator
IDA-PBC	Interconnection and Damping Assignment - Passivity Based Control

Chapter 1

Introduction

The main function of the excitation system is to provide the field current to the field winding of the synchronous generators. Hence initially, dc generator based excitation controllers were used. With the advent of fast acting semiconductor switches like thyristors and IGBTs, static excitation systems were developed that were having very fast response times. Hence after an era of slow acting excitation systems, fast acting excitation systems came mainly with the development of Automatic Voltage Regulators (AVRs). The AVRs were having fast response time; hence they were able to improve the transient stability of the power system. But analysis showed that under heavy loading conditions as well as under weak power system conditions, they provide negative damping torque and stronger synchronizing torque. Hence this resulted into increased oscillations of the rotor of the synchronous machine and hence the loss of synchronism. Thus small signal stability was reduced. In order to mitigate this problem, power system stabilizers (PSS) were developed that provide a positive damping torque component, but the tuning of PSS is an issue although different techniques are suggested in literature.

1.1 Types of Excitation Systems

According to IEEE 421.1 standard, excitation systems are categorized into three types:

1. **DC Excitation:** This is a conventional method of exciting the field windings of synchronous machines. In this method; three machines, namely pilot exciter, main exciter and the main three phase alternator are mechanically coupled and are therefore driven by the same shaft. The pilot exciter is a dc shunt generator feeding the field winding of a main exciter. The main exciter is a separately excited dc generator. The dc output of the main exciter is given to the field winding. They are again sub-categorized as DC1A, DC2A and DC3A.

2. **Static Excitation:** In this method, the excitation power for the main alternator field is drawn from output terminals of the main three phase alternator.

For this purpose, a three phase transformer steps down the alternator voltage to the desired value. This three-phase voltage is fed to the three-phase full converter bridge using thyristors. The firing angle of these thyristors is controlled by means of a regulator which picks up the signal from alternator terminals through potential transformer PT and current transformer CT. The controlled output from thyristor unit is delivered to the field winding of main alternator through brushes and slip rings. They are sub-categorized as AC1A, AC2A, AC3A and AC4A.

3. **Brushless Excitation** In this scheme, prime mover drives the pilot exciter, main exciter and main alternator altogether along with silicon diode rectifiers which are mounted on the same shaft. Pilot exciter is a permanent magnet alternator with permanent magnet poles mounted on the rotor and three phase armature winding on the stator. Hence as the pilot exciter rotates three phase power is generated and this three phase voltages are provided to thyristor controlled bridge rectifier. Due to rectification, the dc output is obtained from ac voltages and hence this dc voltage is supplied to stationary field winding of main exciter. The main exciter has field winding on the stator and the armature winding on the rotor. Thus three phase power is generated on the rotor. Since diode based rectifier is connected on the same shaft of the main exciter having the input from the output of main exciter, hence again rectification occurs and thus dc output voltage is obtained which can be fed to the field winding of the synchronous generator. They are sub-categorized as ST1A, ST2A and ST3A.

Chapter 2

Literature Survey

1. **Francisco P. Demello, Senior Member, IEEE, and Charles Concordia,"Concepts of Synchronous Machine Stability as Affected by Excitation Control,"IEEE Transactions on Power Apparatus and Systems, VOL. PAS-88, NO. 4, APRIL 1969**
   In this paper, the stability of synchronous machines due to small disturbances were studied on a single machine infinite bus through external reactance i.e. of transformer and transmission line. The analysis shown in the paper explains the effects of excitation systems mainly of thyristor type and the necessary conditions for obtaining the stability are explored. For this, the gain of automatic voltage regulators are taken into consideration as the driving for stability and hence is represented in the transfer function of the entire system.
   Hence the criteria for gain of voltage regulators, their effect on synchronizing and damping torques and the modelling of the synchronous machine is discussed. Thus small signal stability is deeply studied.

2. **Gurunath Gurrala and Indraneel Sen,"Synchronizing and Damping Torques Analysis of Nonlinear Voltage Regulators", IEEE Transactions on Power Systems, VOL. 26, NO. 3, August 2011**
   This paper, the relative analysis of the excitation system comprising of (AVR+PSS) and a nonlinear voltage regulator is done. In order to obtain this firstly the modelling of single machine connected to infinite bus through a transformer and transmission line is done and then synchronizing and damping torque components are obatined for both cases. In past of years, a considerable amount of research has been done in designing nonlinear excitation controllers, in order to obtain a better dynamic performance over a wider range of system and operating conditions.
   This paper consists of the performance and analysis of two different topologies basically nonlinear controllers which are based on feedback linearization namely FBLAVR and include automatic voltage regulation giving a better dynamic performance for a SMIB model. Linearizing the nonlinear control laws

along with the SMIB system equations, a Heffron Phillips type of a model has been derived.
This paper analyzes both the nonlinear voltage regulators and the performance as far as small signal stability is concerned. The synchronizing and damping torques and the new constants from modified Heffron-Phillips model are deeply studied.

3. **Gurunath Gurrala, Indraneel Sen Viswanath Talasila and Purnaprajna Mangsuli, "A Novel Approach for Designing Excitatiion Controllers Using the IDA-PBC Technique", IEEE, Conference January 2009**
This paper presents designing of generator excitation controllers using Interconnection and Damping Assignment Passivity Based Control (IDA-PBC) technique that was primarily suggested by Romeo Ortega along with his associates for a Single Machine Infinite Bus (SMIB) system. This approach's applicability on multi-machine system is also analyzed showing some of the very promising results.
In this paper, the transformer bus is taken as the reference and hence Heffron Phillips model is revised accordingly showing the changes mainly on the generator side. For the modified system equations, IDA-PBC is applied to stabilize the system around an operating condition. This design forms a Lyapunov function or an energy function for the modified system. Hence it concentrates on the energy supplied, energy stored and energy dissipated. The control law thus obtained is practically feasible and can be applied directly to multi-machine system without depending on the external system parameters.
In this paper, the proposed controller is tested on a SMIB system and on a 10 generator 39 bus test system. The results obtained are much better than those of the coventional system.

4. **IEEE Standard 421**
IEEE 421.1: This standard provides definitions of elements and commonly used components in excitation systems. It also includes one-line block diagrams of most of the typical type of excitation systems that can be broadly classified into three categories. Thus this standard provides the definitions and broad classification of different type of excitation systems used along with their generalized block diagrams.
IEEE 421.2: This standard mainly deals with the testing procedures of different excitation systems in order to analyze and observe its dynamic performance that are required by electric utilities. This guide also includes criteria and definitions required for the same.
IEEE 421.3: Under this standard, excitation systems are tested for high potential test voltages for sychronous machines and hence the minimum require-

ments are defined. These test voltages are established considering the equipment connection with the exciter power circuit as well as when it is electrically isolated from the same.
IEEE 421.4: This guide mainly focuses on the customer side i.e. the type of specifications that should be provided by and to the purchaser of an excitation system. It also includes narrative descriptions of functions for typical excitation systems. Narrative consists of types of excitation systems and information required for sizing the excitation system.
IEEE 421.5: It recommends the various practices for excitation system models to carry out power system stability studies.

5. **A. Godhwani, M.J. Basler, "A Digital Excitation Control System for Use on Brushless Excited Synchronous Generators", IEEE Transactions on Energy Conversion, Vol. 11, No. 3, September 1996**

   This paper describes a new approach for obtaining the stability parameters for small to medium sized generators that have varying effect on overall system stability. Digital Excitation Control System utilizes a discrete Proportional, Integral and Derivative (PID) control algorithm. The test results are also presented for direct design (Pole Placement) method for determing PID parameters.

6. **P.M. Anderson and A.A. Fouad, "Power System Control and Stability", A. John Wiley and Son, Inc., Publication, 2003.**
   Detailed learning about power system stability- elementary analysis, small signal stability analysis of power system.

7. **Allen J. Wood and Bruce F. Wollenberg, "Power Generation, Operation and Control", John Wiley and Sons, Inc., Publication, 2013.**
   The state estimation methods were mainly studied from the book and accordingly implemented. Mainly the Weighted Least Square Estimation was studied and implemented.

8. **Ramanujam R, "Power System Dynamics: Analysis and Simulation", Prentice Hall of India, Publication, 2009.**
   The analysis for SMIB and multimachine systems are studied along with detailed analysis on AVRs and PSS. Also the effect of inclusion of SVC on small signal stability is well analyzed. Also the concepts of multimachine system are studied.

9. **K R Padhiyar, "Power System Dynamics: Stability and Control", BS Publications, Publication, 2008.**

The concepts of Synchronous machine modelling, analysis of SMIB system and design of PSS were studied. Due to the inclusion of FACTs devices, the small signal stability was analyzed.

10. **Romeo Ortega, Martha Galaz, Alessandro Astolfi, Yuanzhang Sun, and Tielong Shen,"Transient Stabilization of Multimachine Power Systems with Nontrivial Transfer Conductances,"IEEE Transactions on Automatic Control, VOL.50, NO. 1, pp. 60-75, JANUARY 2005**
In this paper Lyapunov function is used to solve the transient stability problem for a multimachine system using interconnection and damping assignment passivity based control method introduced by R. Ortega.

11. **Romeo Ortega, Arjan van der Schaft, Bernhard Maschke, and Gerardo Escobar,"Interconnection and Damping Assignment Passivity Based Control of Port Controlled Hamiltonian Systems,"Automatica 38, 585-596, 2002**
IDA-PBC method is introduced in this paper which can be utilized to design robust controllers for most of the electomechanical applications since utilizes the energy function of the system.

Chapter 3

Simulations of Static Excitation System and H-P constants

The static excitation systems namely Full bridge thyristor based and Full bridge diode based rectifier with Buck converter were simulated in MATLAB simulation package. After that simulation was made to calculate the Heffron-Phillips constants as well as modified model by Reference [2].

3.1 Thyristor Excitation System

Here six pulse thyristor based full bridge rectifier is used that takes the ac power as input from the generator terminals. Here the firing angle is kept as 0 degree. It can be observed from Fig. 3.2 that some amount of harmonic content is introduced. In order to reduce the ripple content in output and harmonic introduction one can opt for 12 pulse thyristor but it is not economical.

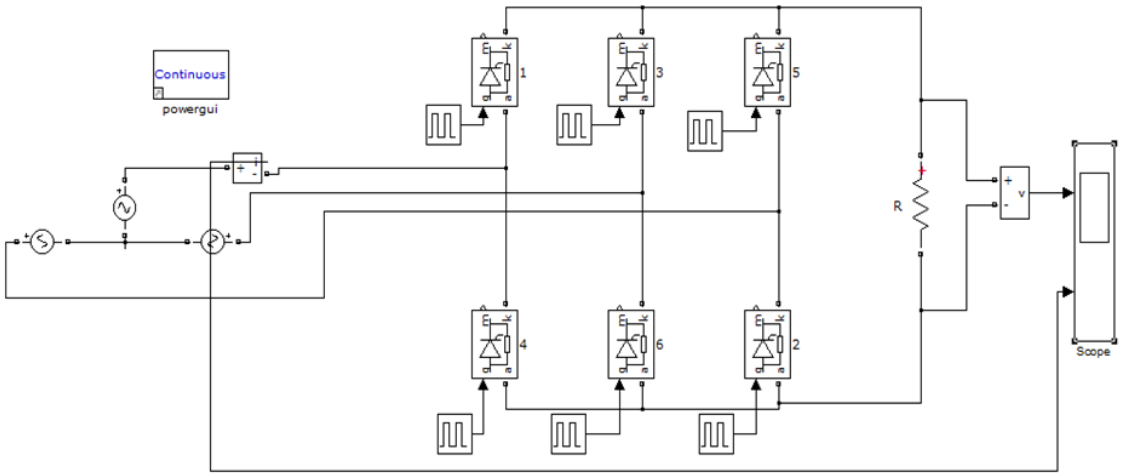

Figure 3.1: Thyristor Full Bridge Rectifier

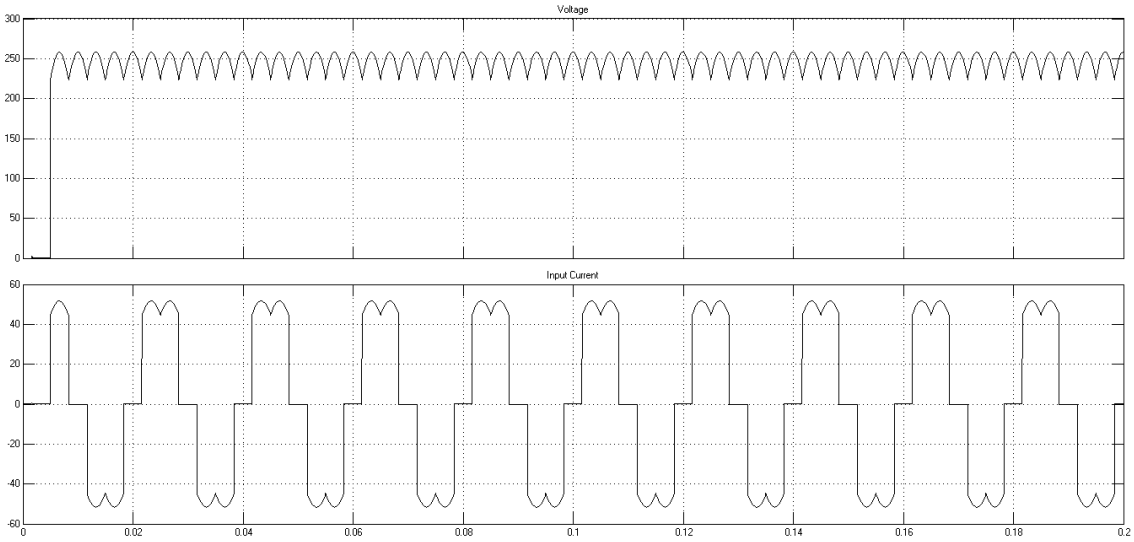

Figure 3.2: Output Voltage and Input Current for Thyristor Rectifier. [X-axis: 0.02 s/div.; Y-axis: Plot1: 50 V/div., Plot2: 20 A/div.]

3.2 Diode Full bridge rectifier with Buck converter excitation system

In this type, a simple diode based full bridge rectifier is used which is connected with Buck converter through an IGBT switch. The duty cycle of this IGBT can be controlled and hence accordingly the appropriate voltage levels can be obtained. In this case the control is much easier. Generally the inductance for the buck converter is not provided externally because of the high inductance of field winding.

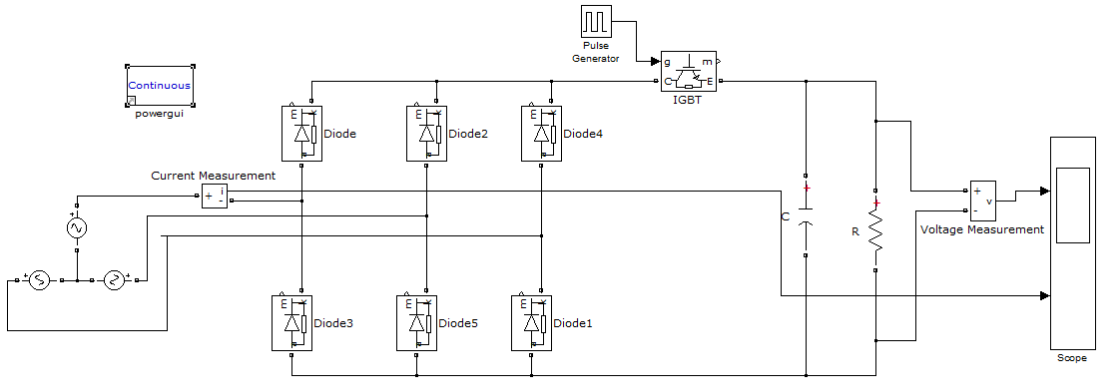

Figure 3.3: Diode Full Bridge Rectifier with Buck Converter

Fig 3.4 shows that a triangular signal wave is compared with a constant dc value

and when the magnitude of carrier signal is smaller than constant DC value, a pulse is generated. Thus by varying either of the two quantities, the pulse width can be varied and hence the switching times or the duty cycle of IGBT is changed. The output of this type of excitation system is shown in Figure 3.5 where the duty cycle is kept 90%. It can be observed that the notches are seen in the output voltage waveform and also tremendous amount of harmonics are injected into the system because of the highly non-linear current.

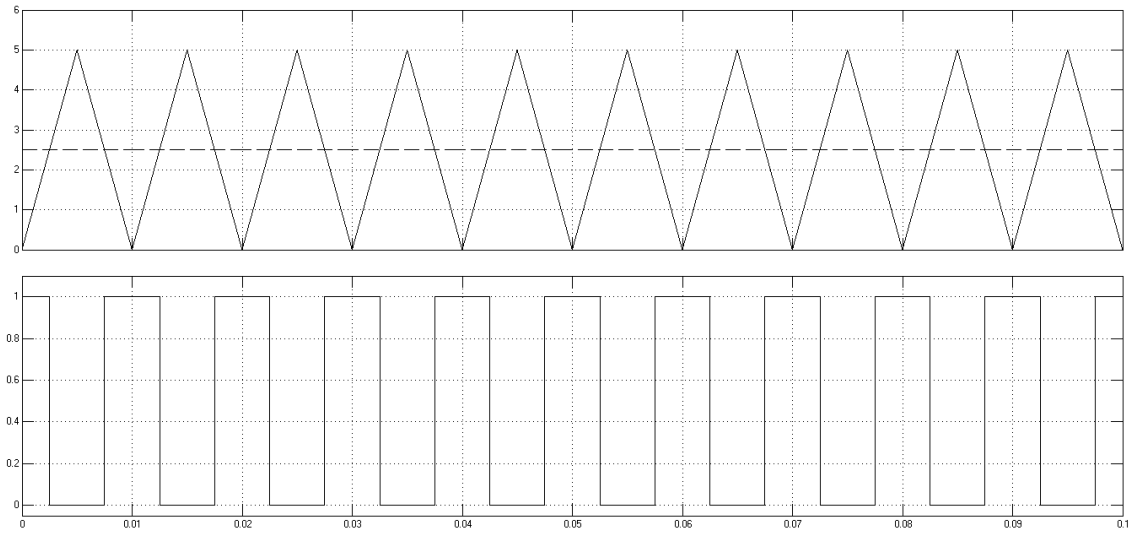

Figure 3.4: Pulses for IGBT Control. [X-axis: 0.01 s/div.; Y-axis: Plot1: 1 V/div., Plot2: 0.2 pu/div.]

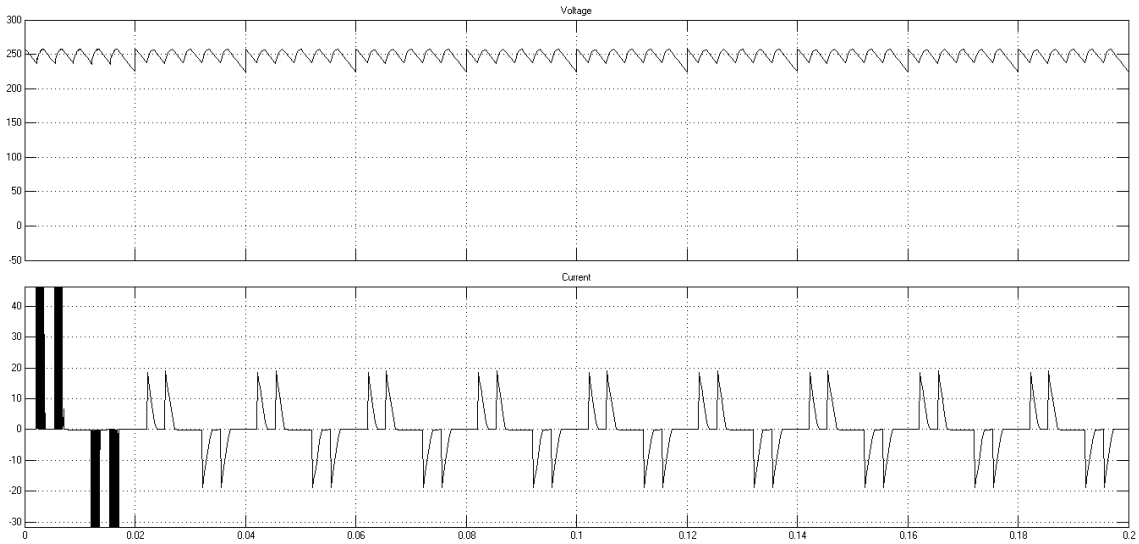

Figure 3.5: Output of Diode Full bridge Type Excitation System. [X-axis: 0.02 s/div.; Y-axis: Plot1: 50 V/div., Plot2: 10 A/div.]

3.3 Heffron-Phillips constants model

The simulation model was created to calculate the Heffron Phillips constants[1] for all scenarios as shown in Fig. 3.6. Along with them the constants as GD, G5 and G6 as defined in [2] can also be calculated. These are obtained from the modelling of synchronous generators and its analysis on Single Machine Infinite Bus. The equations are derived in three parts; namely 1) Rotor Mechanical Torque Equations, 2) Flux Decay model and 3) Excitation system model. The constants K1, K2, K3, K4 and K6 are generally positive in wide operating range. But the constant K5 can be positive or negative according to the system conditions and loading. For strong system and lightly loaded condition, it is positive but for weak system conditions and heavily loaded conditions this constant becomes negative. This results in increased negative damping torque and hence the system moves out of synchronism although synchronizing torque is high. Hence the external reactance should be small.

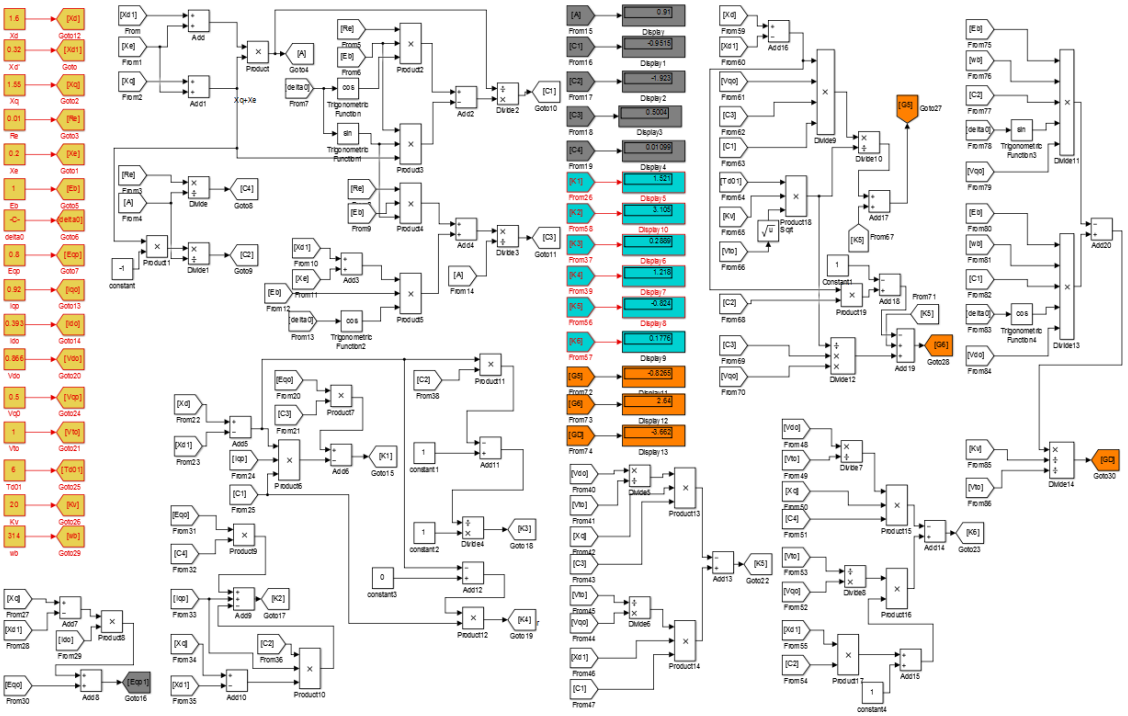

Figure 3.6: Heffron Phillips Constants Model

Chapter 4

Excitation system response in a Radial System

In order to simulate this condition the circuit breaker at the infinite bus end in a Single Machine Infinite Bus (SMIB) is operated at the starting point of time only. Initially both the loads are connected. At time t=0.5 seconds, load 2 is disconnected. At time t=1.2 seconds, three phase fault is created on line 2 which persists for 10 cycles and then cleared out. Accordingly the results are observed with both excitation system provided by MATLAB and the Feedback Linearization AVR proposed by Mak[2]. Fig 4.1 shows the model prepared in MATLAB that can be used as both radial and SMIB system. Fig. 4.2 shows the voltage, current, rotor mechanical angle and fault current. Fig. 4.3 shows the effect in Park's voltages vd, vq, terminal voltage and load angle. The instant of fault clearing is zoomed in Fig. 4.4 and it can be observed that 5 to 6 cycles are required to stabilize the voltage. The excitation response is shown in Fig. 4.5. Feedback linearization AVR (FBLAVR) proposed by Mak is implemented in Fig. 4.6. For this type of excitation control the similar results are again obtained. It can be observed that time required to reach the rated voltage in FBLAVR is lesser than the conventional excitation system. Hence transient stability is better as far as the radial systems are considered. Also it requires only 3 to 5 cycles to stabilize the voltage which is much lesser than the previous case.Gain of FBLAVR is 20 and that of MATLAB excitation system is 14.

Data are given as under:
Generator: 600 MVA, 22 kV, 3000 rpm. Xd=1.65, Xd'=0.25 Xd''=0.02, Xq=1.59, Xq'=0.46, Xq''=0.2, Xl=0.14 pu. Stator resistance Rs=0.0045 ohm. Inertia coeffecient H=0.8788, Pole pairs=1, Tdo'=4.5, Tqo'=4.5, Tdo''=0.04, Tqo'=0.67, Tqo''=0.09.
Transformer: 600 MVA, 22/500 kV
Load1= 300+j120 MVA
Load2= 100+j40 MVA
Infinite bus voltage= 500 kV

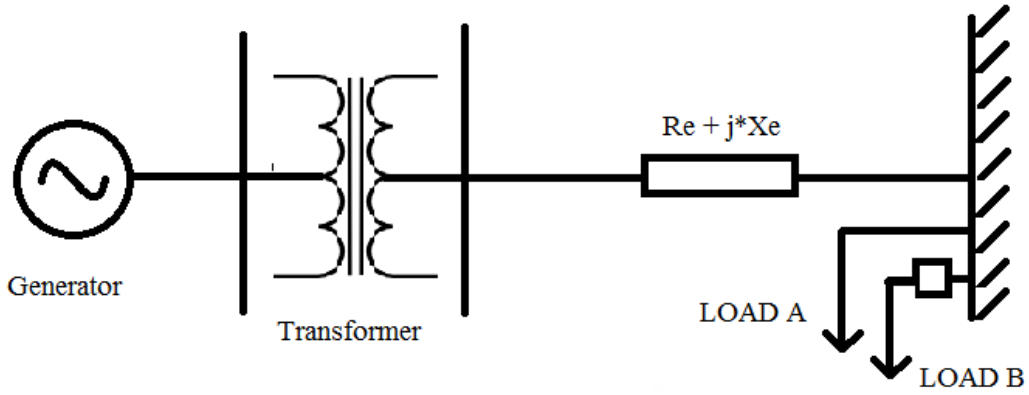

Figure 4.1: Single Machine Infinite Bus

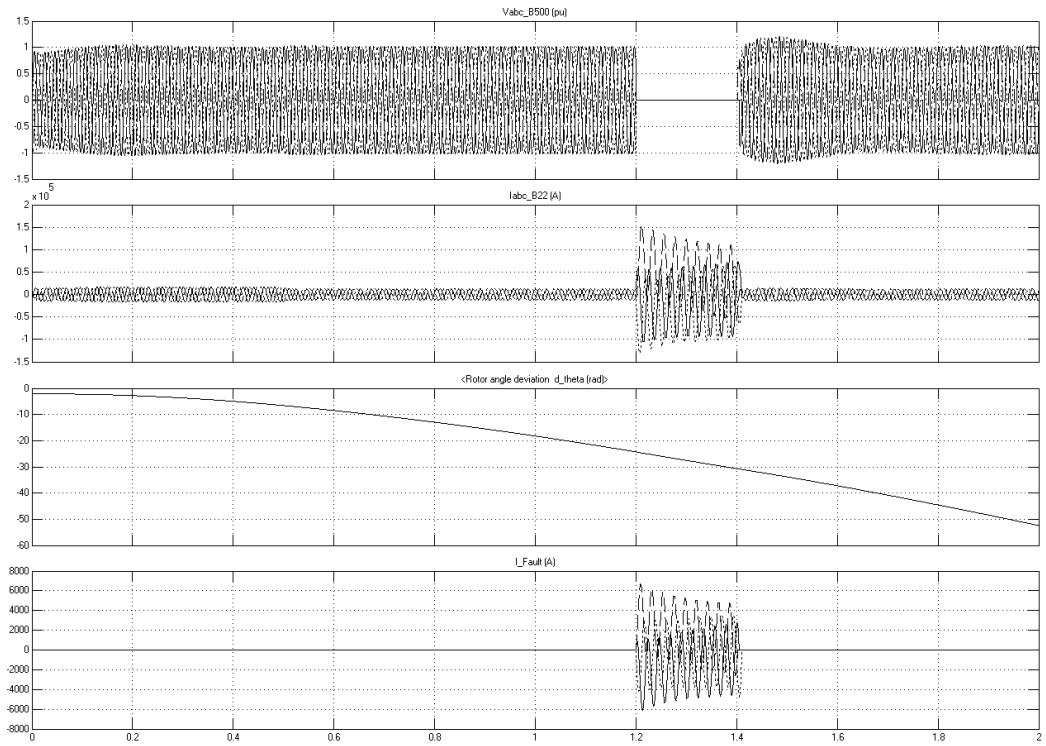

Figure 4.2: Voltage, Current, Rotor Mechanical Angle, Fault Current. [X-axis: 0.1 s/div.; Y-axis: Plot1: 0.5 pu/div., Plot2: 50 kA/div., Plot3: 10 rad/div., Plot4: 2 kA/div.]

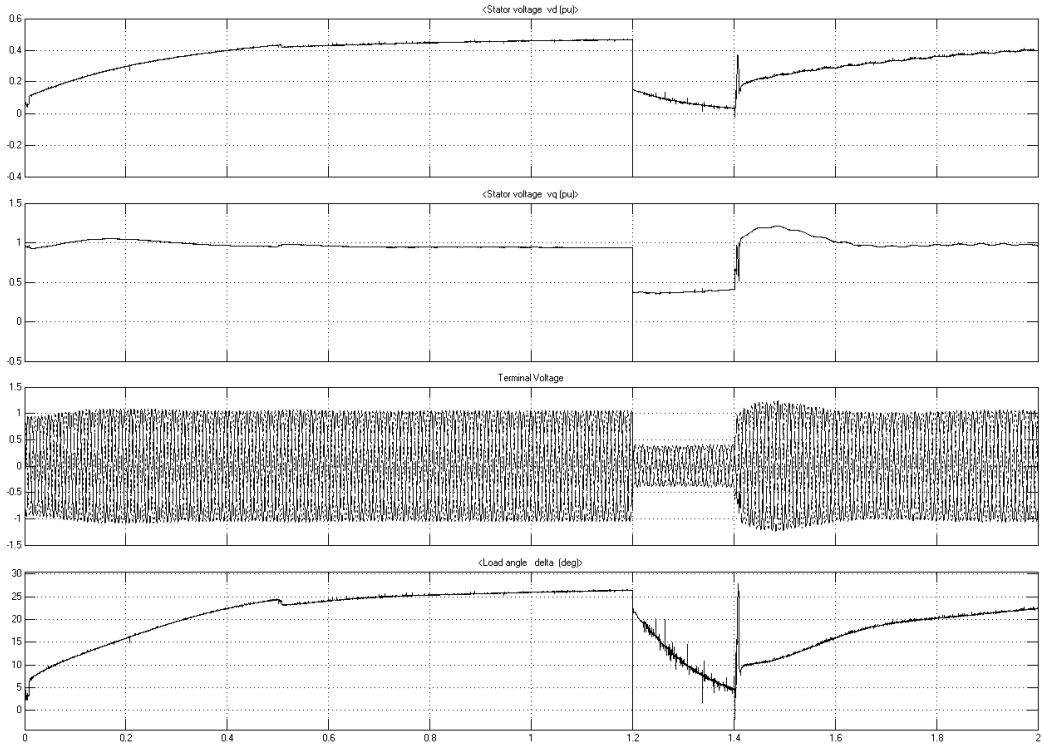

Figure 4.3: V_d, V_q, Terminal Voltage(pu) and Load Angle(degree)

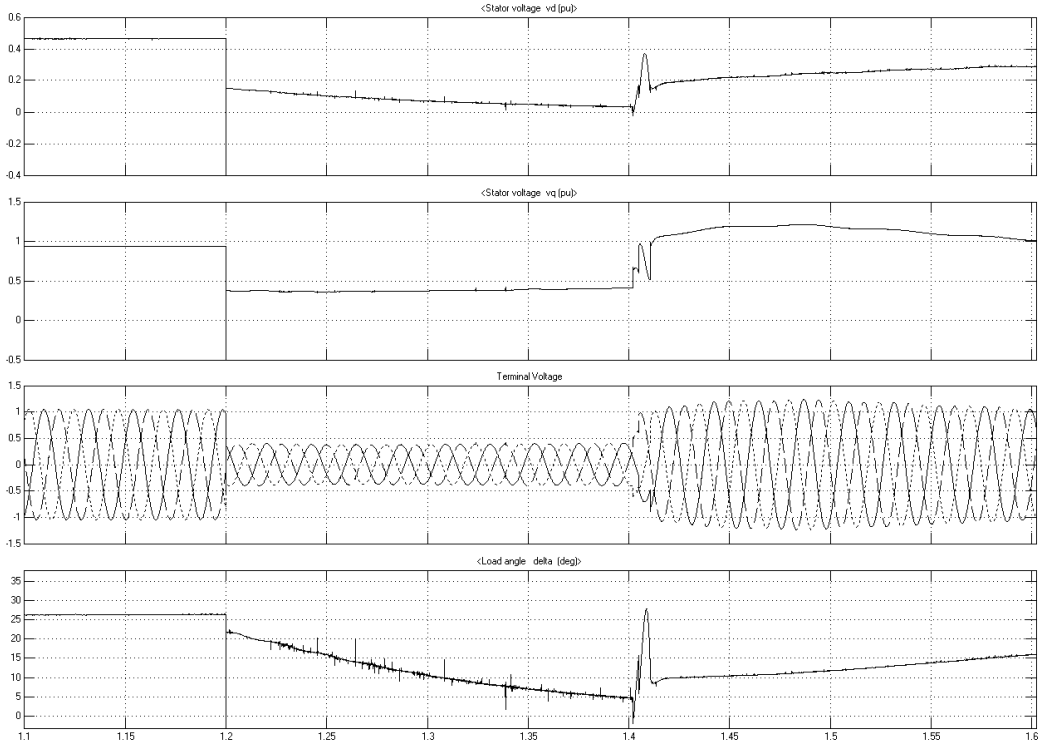

Figure 4.4: V_d, V_q, Terminal Voltage(pu) and Load Angle(degree)

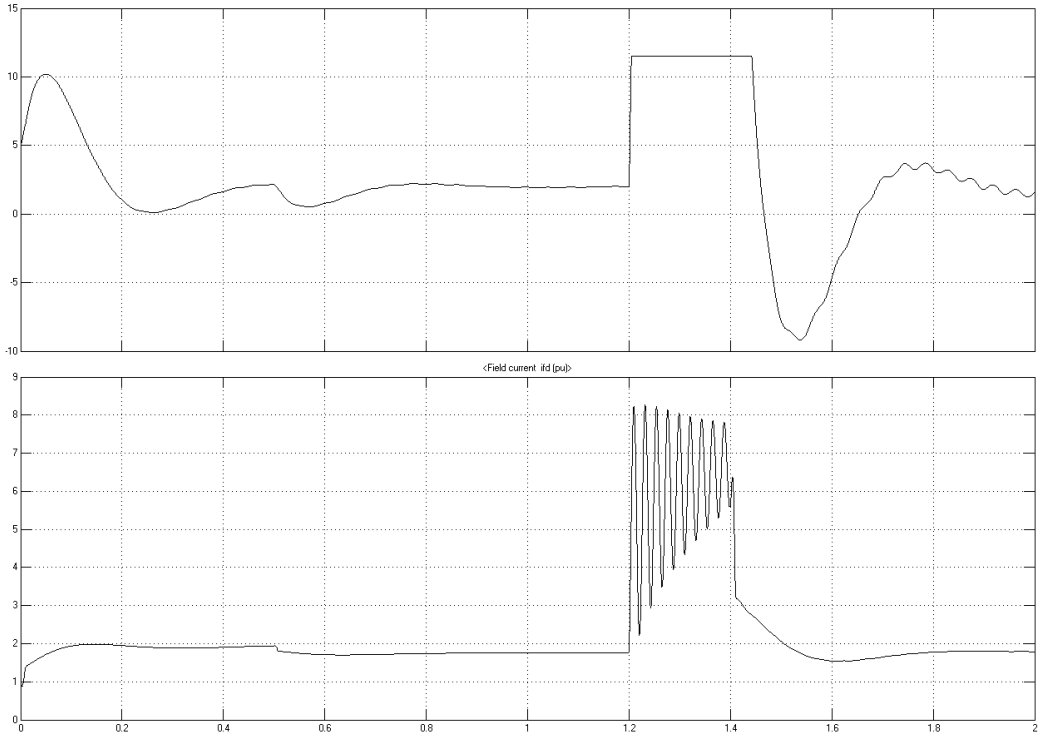

Figure 4.5: MATLAB Excitation System Response under Radial Condition [X-axis: 0.2 s/div.; Y-axis: Plot1: 5 pu/div., Plot2: 1 pu/div.]

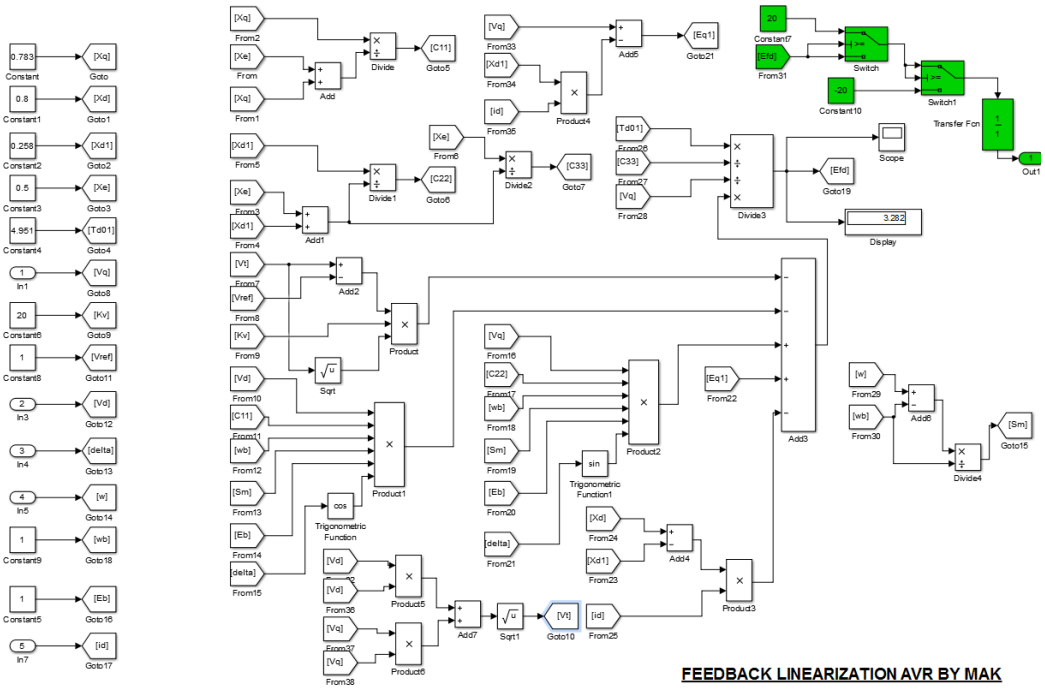

Figure 4.6: Feedback Linearization AVR

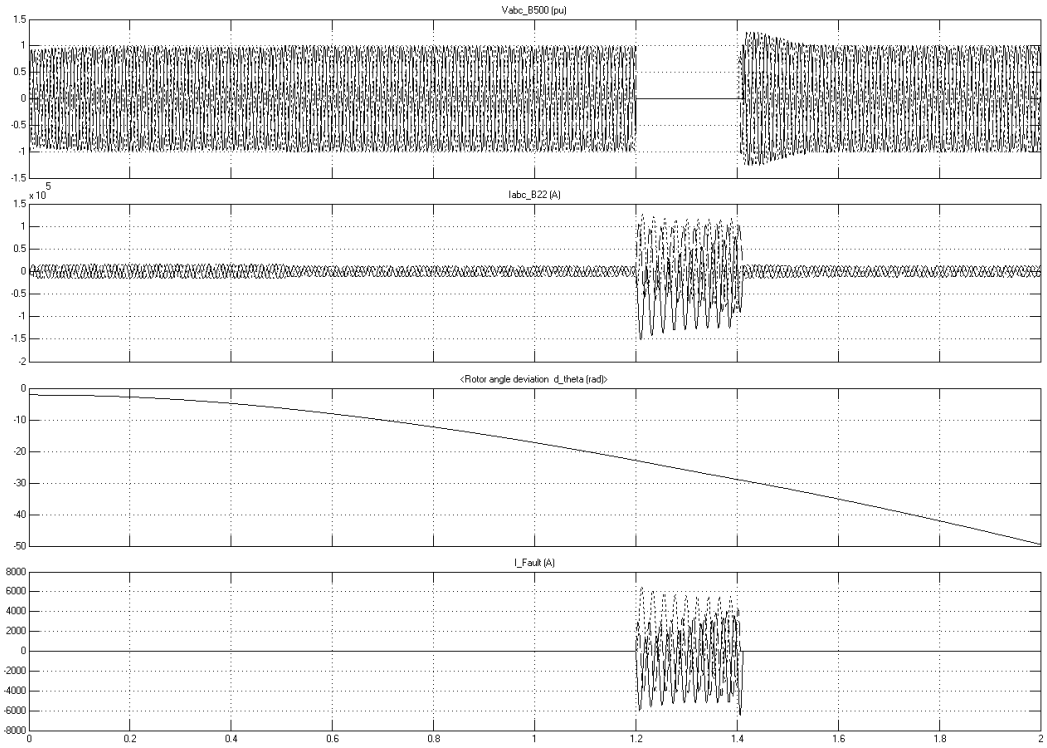

Figure 4.7: Voltage, Current, Rotor mechanical angle, Fault current

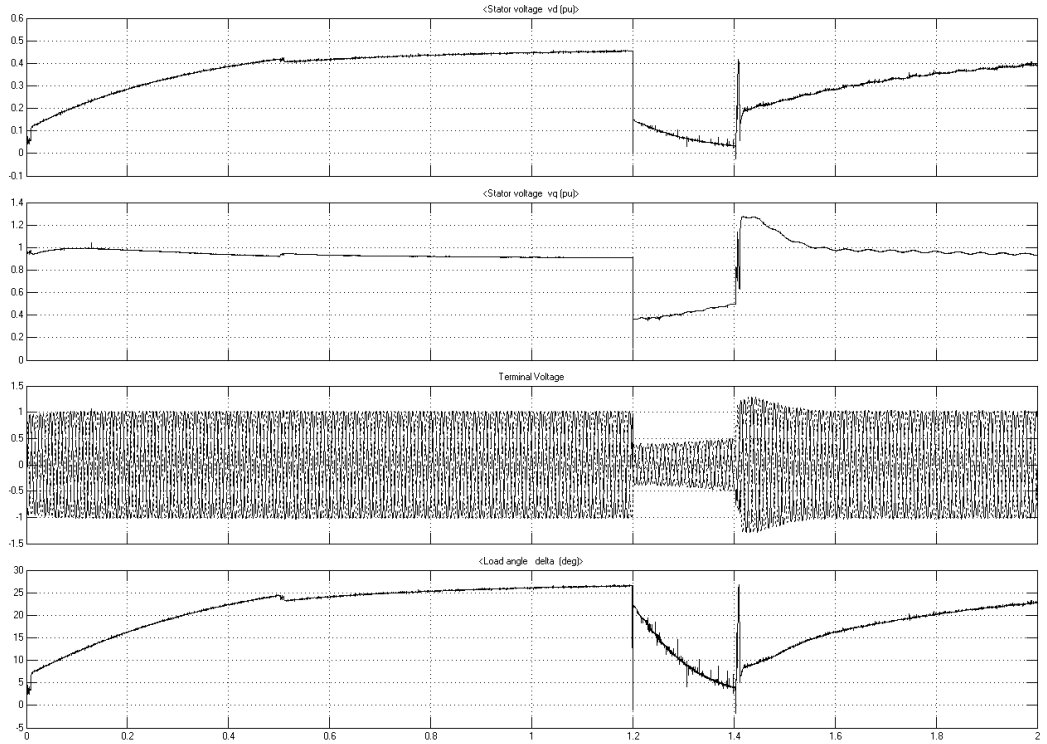

Figure 4.8: V_d, V_q, Terminal Voltage(pu) and Load Angle(degree)

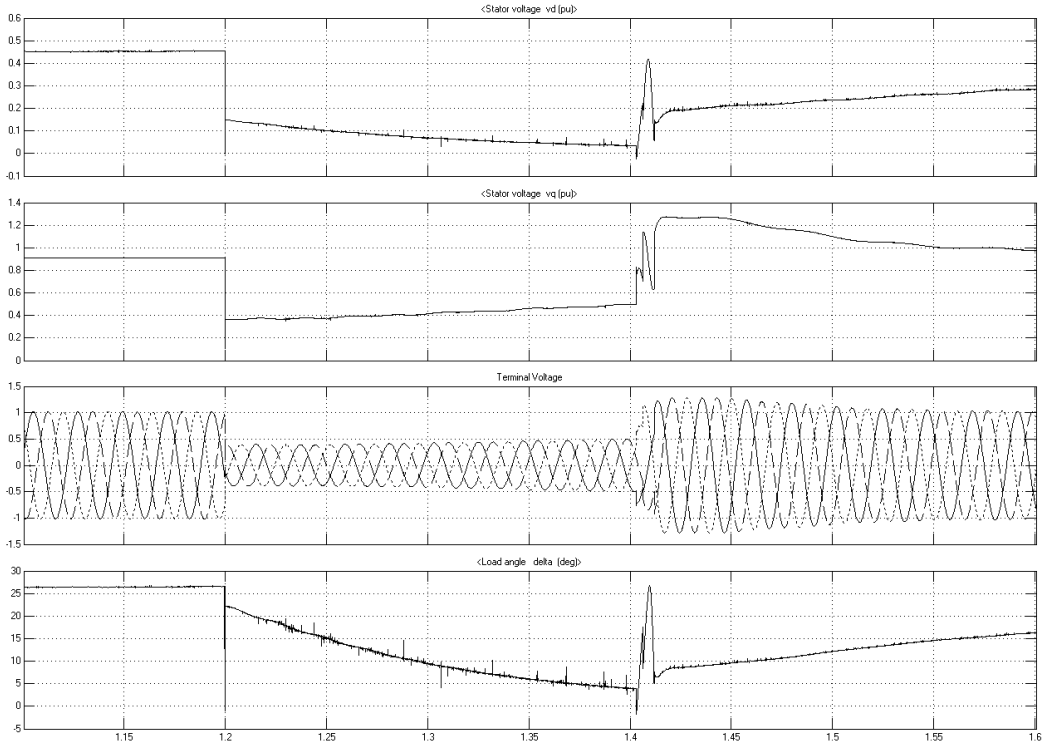

Figure 4.9: V_d, V_q, Terminal Voltage(pu) and Load Angle(degree)

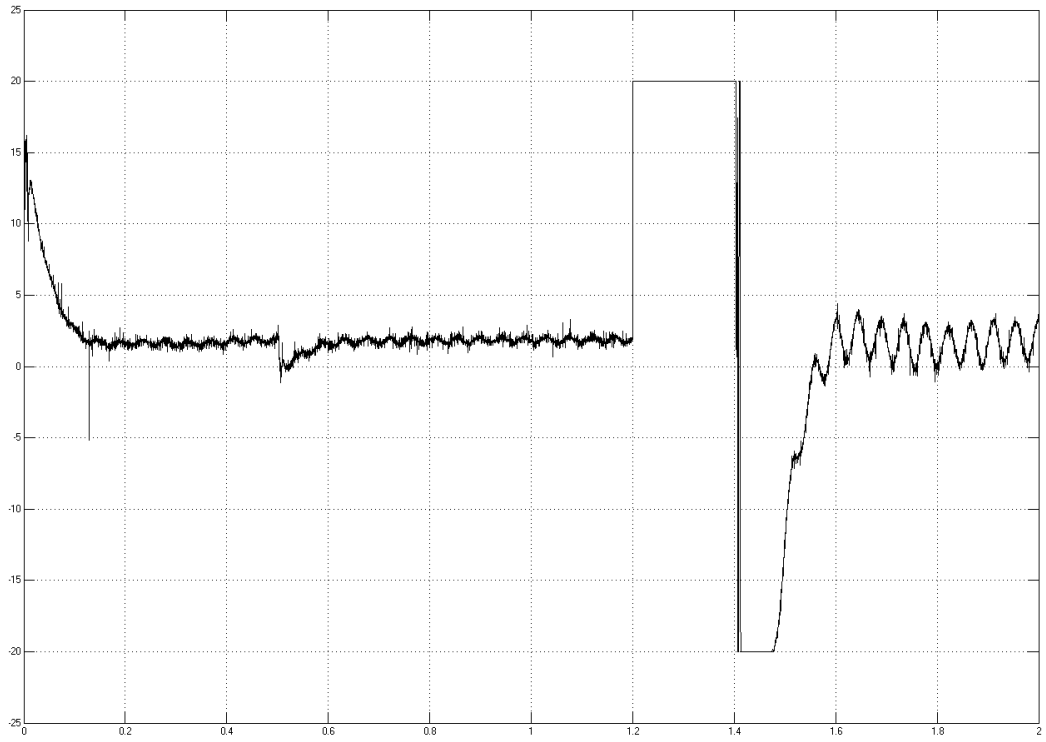

Figure 4.10: Excitation Voltage Response of FBLAVR under Radial Condition[X-axis: 0.2 s/div.; Y-axis: 5 pu/div.]

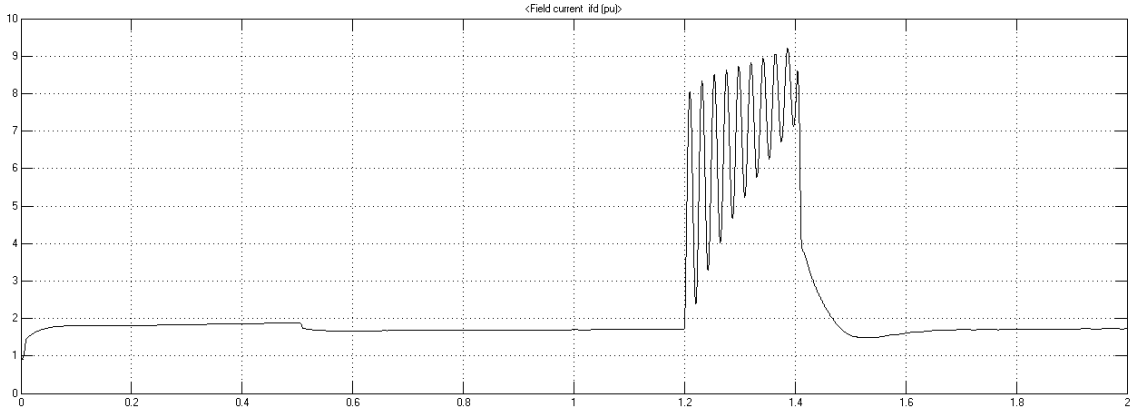

Figure 4.11: Field Current FBLAVR. [X-axis: 0.2 s/div.; Y-axis: 1 pu/div.]

Chapter 5

Excitation System Response in SMIB system

Infinite bus means the bus where voltage and frequency are constant ideally. Practically if the generation is less than or equal to 1 percent of the total capacity of the bus then that bus can be called as the infinite bus. Similar operations like those in Radial conditions are carried out under this case by keeping the circuit breaker closed at the infinite bus end. The results are observed under both the cases. The results obtained under this case are similar to that of radial systems but comparatively the voltages are balanced much faster in both the cases compared to that for radial systems. But the transient stability is slightly better in this case also for FBLAVR. Fig. 5.1 to Fig. 5.4 are for excitation system provided in MATLAB while Fig. 5.5. 50 fig. 5.9 are for the FBLAVR. Gain of FBLAVR is 20 and that of MATLAB excitation system is 14.

Data are given as under:
Generator: 600 MVA, 22 kV, 3000 rpm. Xd=1.65, Xd'=0.25 Xd''=0.02, Xq=1.59, Xq'=0.46, Xq''=0.2, Xl=0.14 pu. Stator resistance Rs=0.0045 ohm. Inertia coefficient H=0.8788, Pole pairs=1, Tdo'=4.5, Tqo'=4.5, Tdo''=0.04, Tqo'=0.67, Tqo''=0.09.
Transformer: 600 MVA, 22/500 kV
Load1= 300+j120 MVA
Load2= 100+j40 MVA
Infinite bus voltage= 500 kV

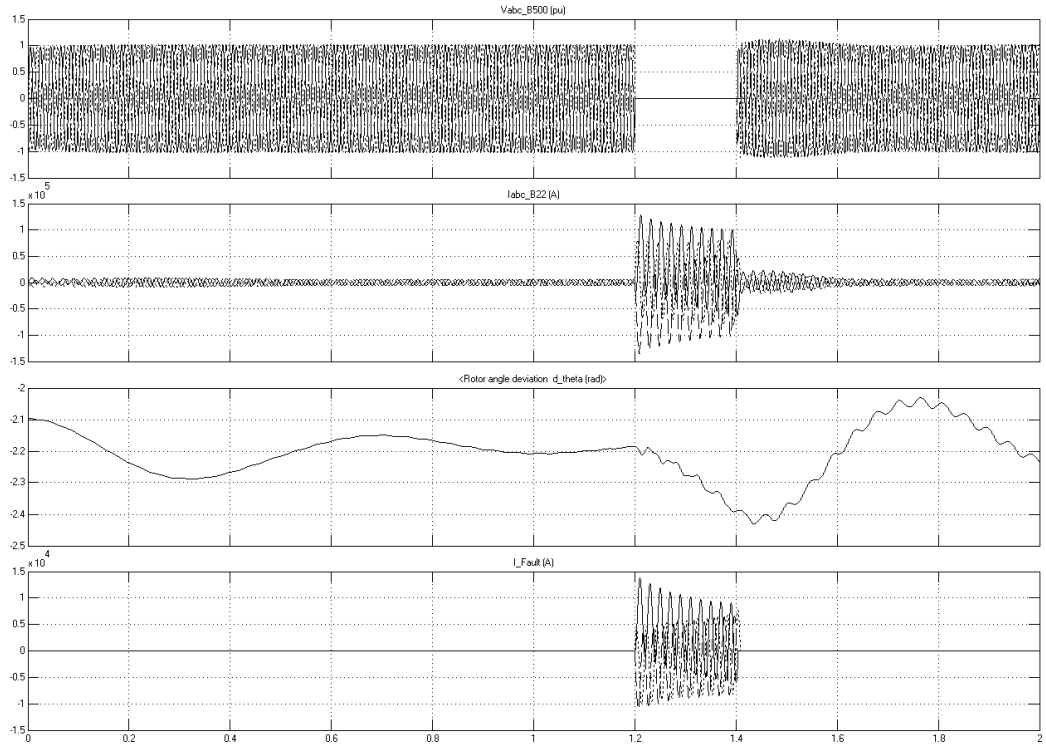

Figure 5.1: Voltage, Current, Rotor mechanical angle, Fault current

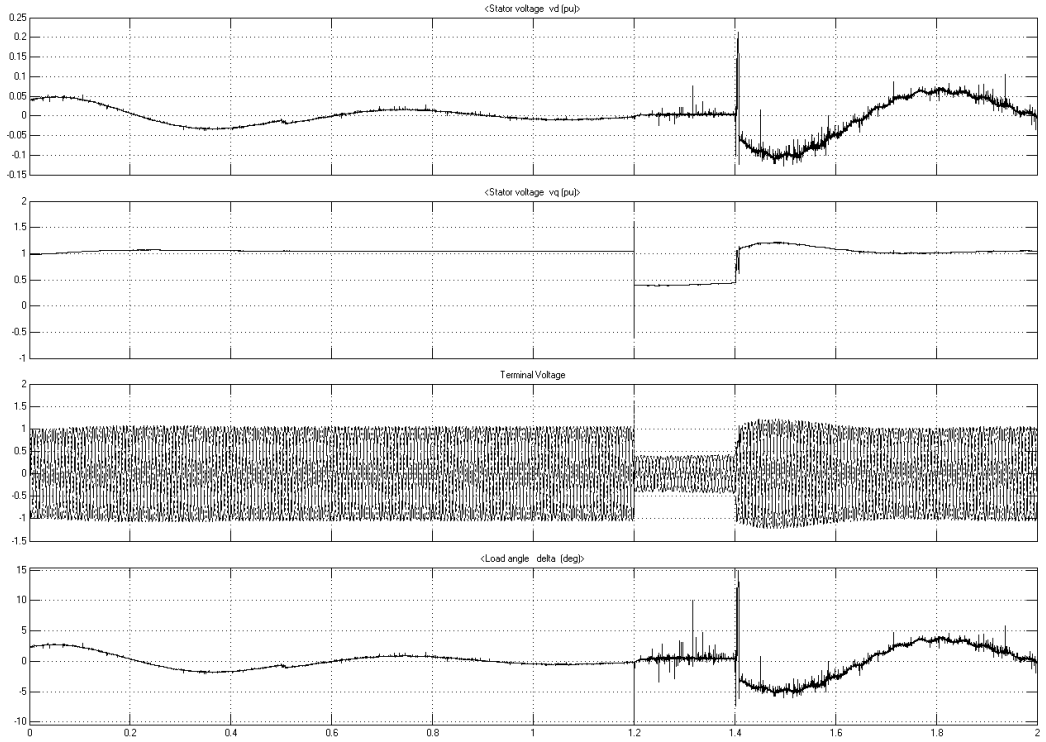

Figure 5.2: V_d, V_q, Terminal Voltage(pu) and Load Angle(degree)

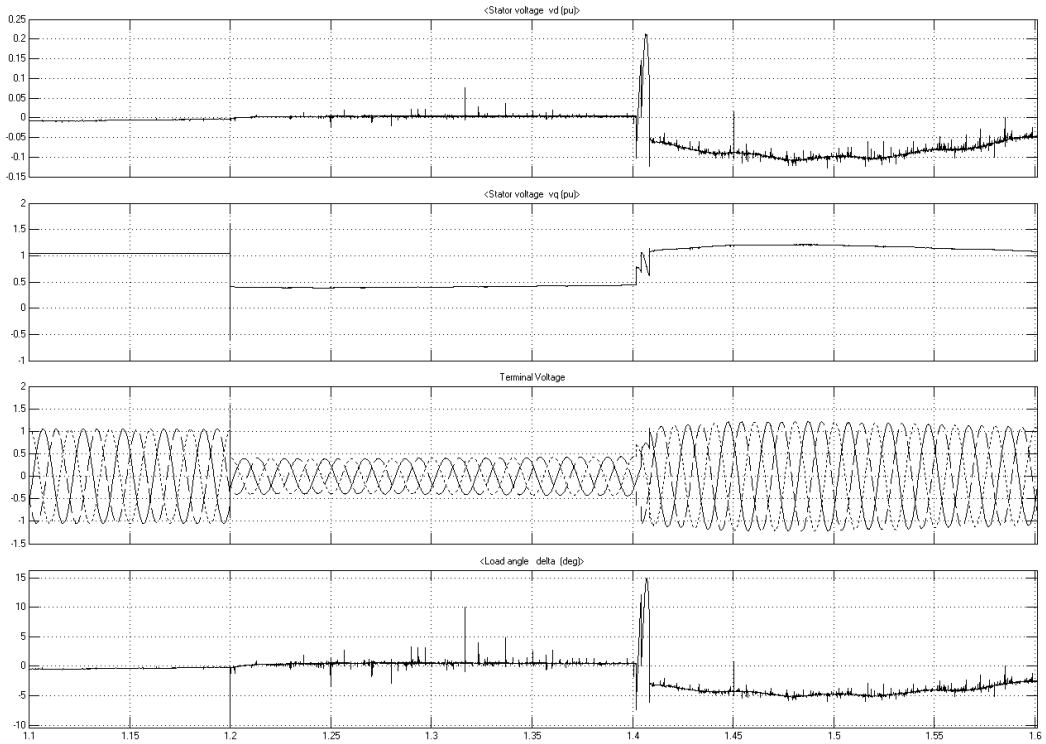

Figure 5.3: V_d, V_q, Terminal Voltage(pu) and Load Angle(degree)

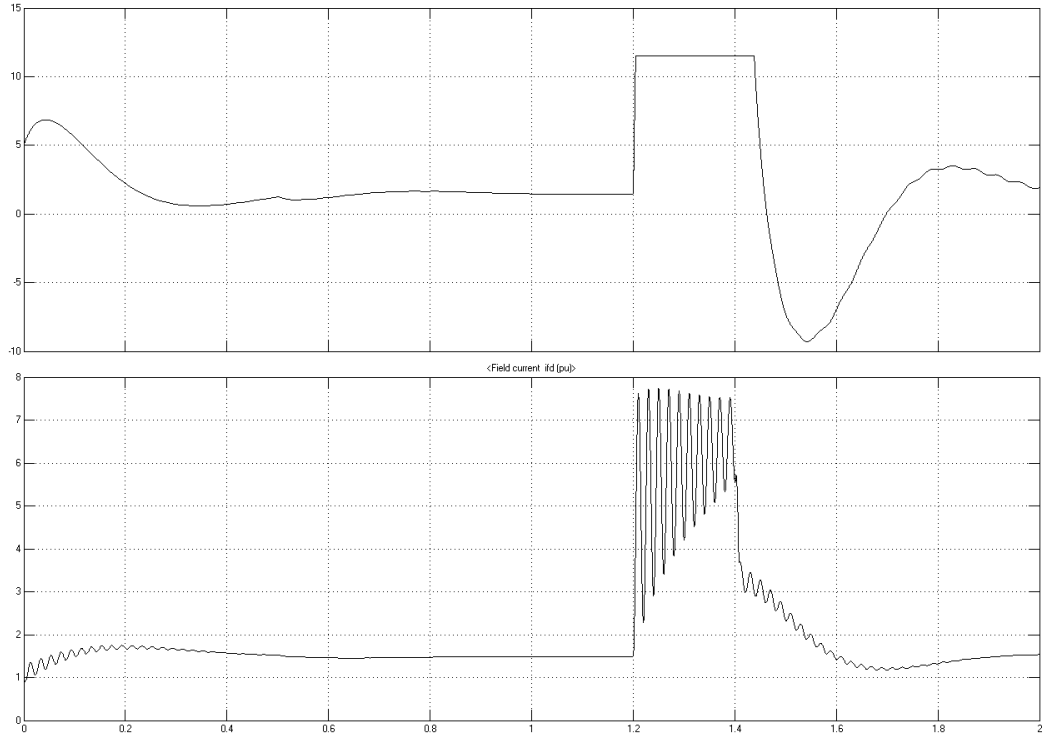

Figure 5.4: MATLAB Excitation System Response in SMIB. [X-axis: 0.2 s/div.; Y-axis: Plot1: 5 pu/div., Plot2: 1 pu/div.]

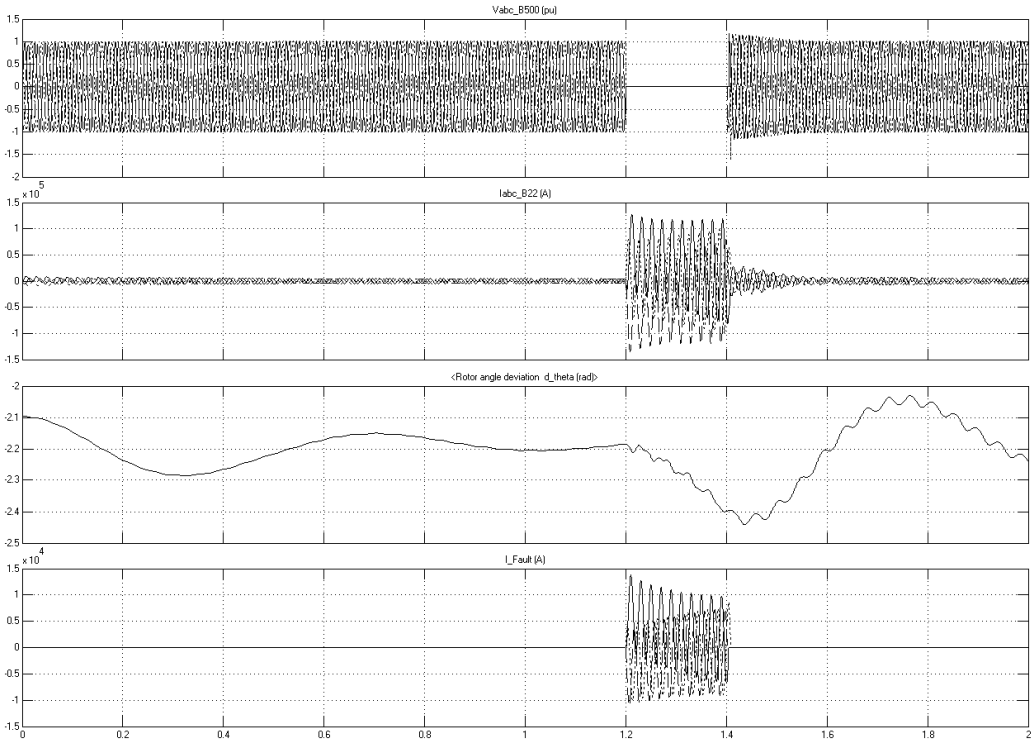

Figure 5.5: Voltage, Current, Rotor Mechanical angle, Fault Current

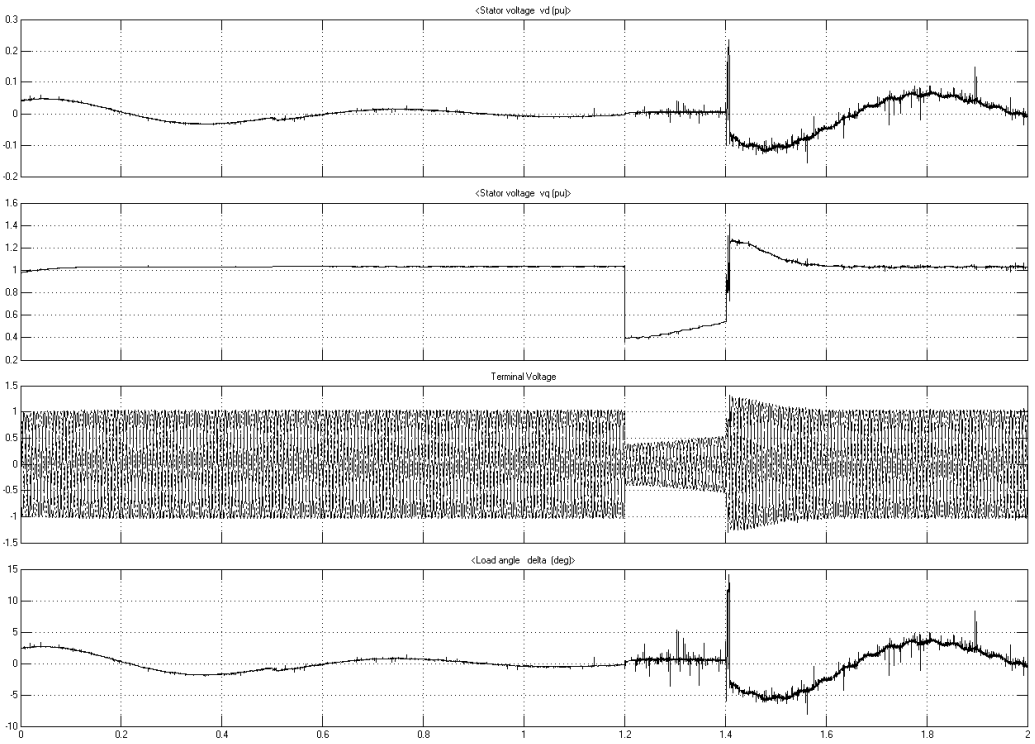

Figure 5.6: V_d, V_q, Terminal Voltage(pu) and Load Angle(degree)

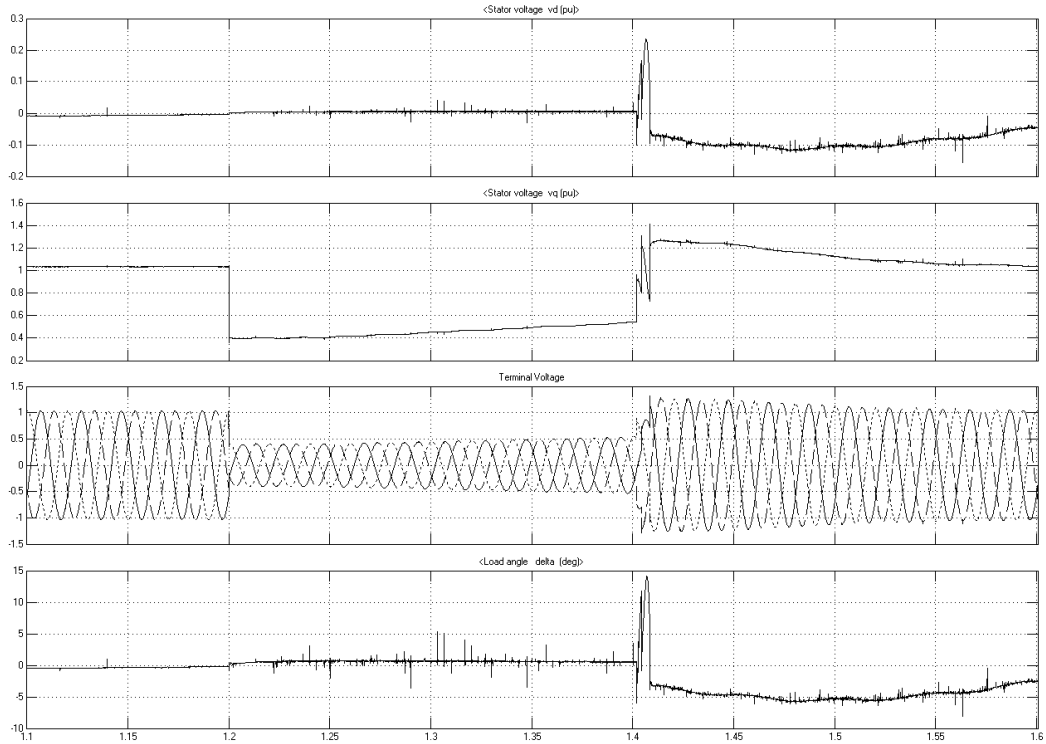

Figure 5.7: V_d, V_q, Terminal Voltage(pu) and Load Angle(degree)

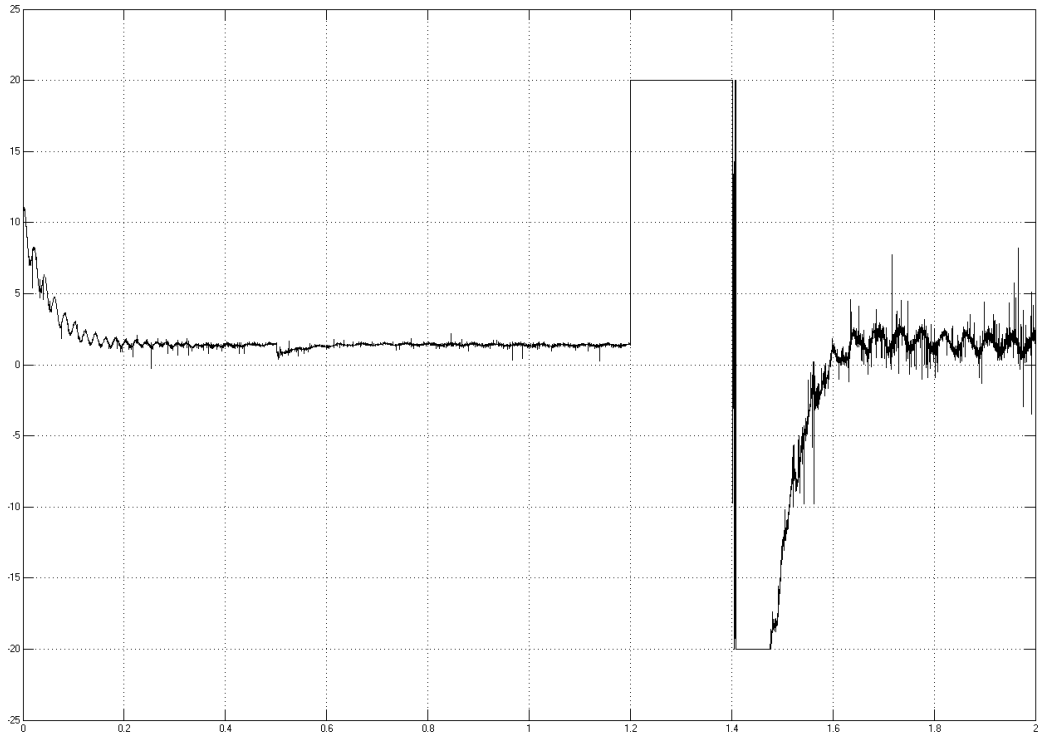

Figure 5.8: Excitation Voltage Response of FBLAVR under Radial Condition. [X-axis: 0.2 s/div.; Y-axis: 5 pu/div.]

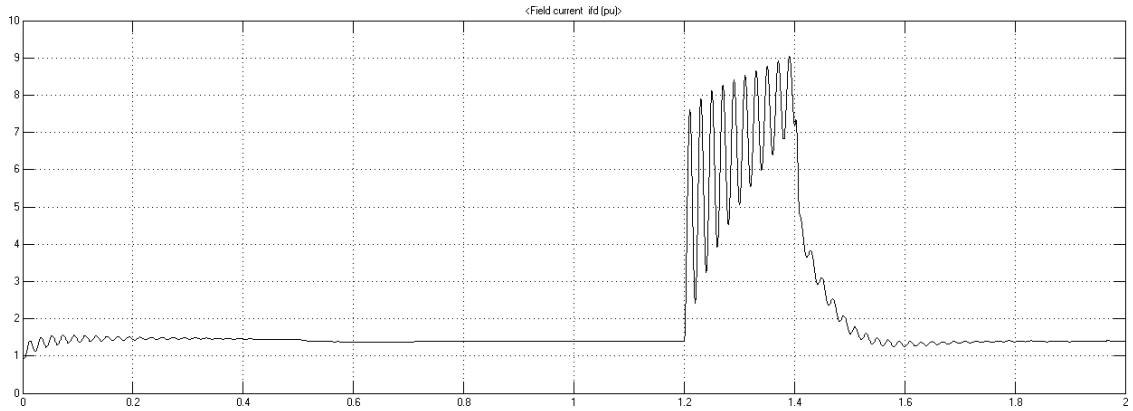

Figure 5.9: Field Current FBLAVR. [X-axis: 0.2 s/div.; Y-axis: 1 pu/div.]

Chapter 6

Implementation of IDA-PBC control

Interconnection and Damping Assignment Passivity Based Control (IDA-PBC) is a technique developed by R. Ortega[11] for control systems and its application for designing a generator excitation control is implemented in this chapter as suggested by Gurunath Gurrala[3]. This technique is compared with AVR and FBLAVR which were implemented in chapter 4 and 5. In this technique transformer secondary voltage is taken as reference and the analysis is done considering the same.

The SMIB system of fig. 4.1 is considered in this case also with only one load equal to 500+j150 MVA connected in the system. The simulation is done for 8 seconds, but the results shown are for the time duration between 1 and 6 seconds. Initially the system works on no load for 1.5 s. Afterwards the load is connected to the system and excitation response as well as power oscillations are observed. The fault is created at 4 s for 20 ms and similar observations are taken.

Fig. 6.1 and 6.2 shows the excitation response of AVR and IDA-PBC respectively. It is observed that during the fault condition the AVR provides the field forcing to maintain the system stable during this transient condition. While IDA-PBC do not provide any field forcing during this condition. Thus it may result into transient stability. While according to the change in terminal voltage and power oscillations IDA-PBC do provide a better response.

Fig 6.3 and 6.4 shows the active and reactive power response for AVR and IDA-PBC control respectively. It can be observed that if the load is connected at infinite bus at 1.5 seconds, very less effect is observed on synchronous generator as was expected. When fault occurs on the transformer secondary bus and then removed, power oscillations are observed especially in active power. These power oscillations are higher in the case of AVR approximately 5-6 cycles. While for the same disturbance in IDA-PBC case the power oscillations are damped out much before i.e. approximately in 3-4 cycles. Thus the power oscillations get sufficient damping in the case of IDA-PBC.

Fig. 6.5 and 6.6 shows the terminal voltage and rotor speed during the same

conditions. In AVR case, the voltage shoots up as soon as the fault is cleared and then lowers down to a stable value. While in case of IDA-PBC control, the voltage never shoots up but get stabilizes slowly. Thus the transient stability provided by AVR is better. But as far as the rotor speed response is concerned, it similar to the response of active power in both the cases clearly showing that it gets stabilized sooner in case of IDA-PBC. Similar observations can be done in case of fig. 6.5 and 6.6. Thus it can be concluded that AVR provides a better transient stability due to the field forcing capability and faster response while IDA-PBC provides a much better small signal stability. Since it is necessary to provide field forcing during fault conditions hence IDA-PBC cannot be implemented individually. But based on the responses of both, [AVR+IDAPBC] can be implemented instead of [AVR+PSS] based on the terminal voltages. It is a well known fact that during fault conditions the voltage gets reduced by a large value. Hence if terminal voltages are with in the prespecified values (maybe 2%) then IDA-PBC is implemented and if terminal voltage goes out of this range then AVR can be implemented. Thus transient stability during large disturbances while small signal stability during small disturbances both can be obtained easily.

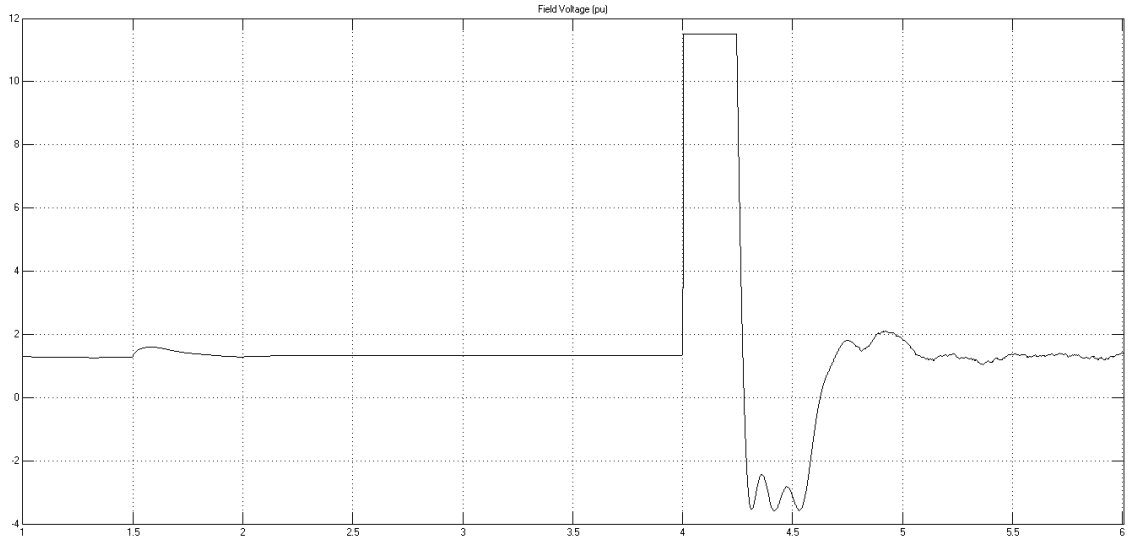

Figure 6.1: Excitation response of AVR. [X-axis: 0.5 s/div.; Y-axis: 2 pu/div.]

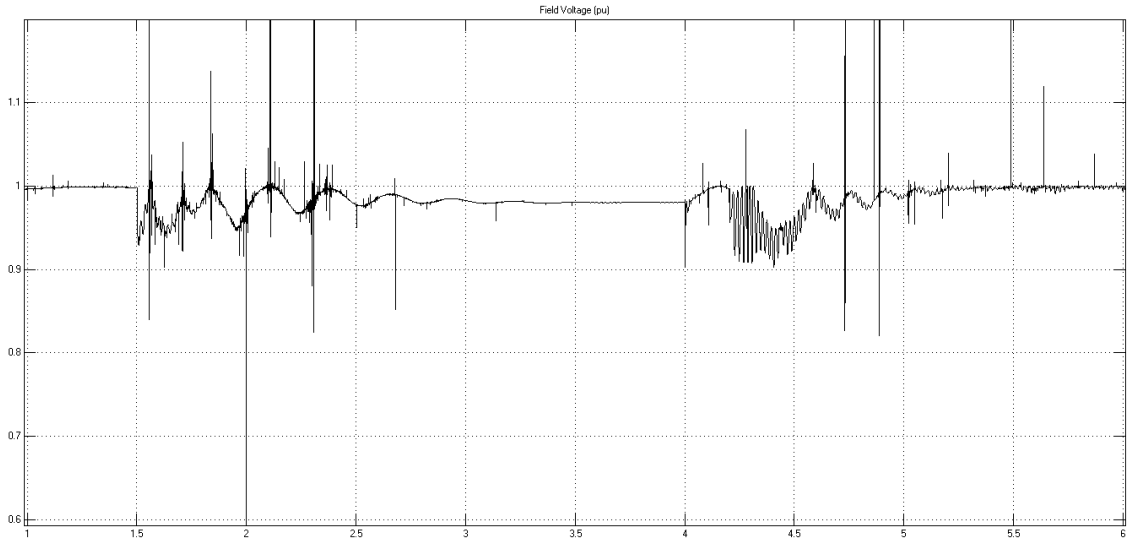

Figure 6.2: Excitation Response for IDA-PBC case. [X-axis: 0.5 s/div.; Y-axis: 0.1 pu/div.]

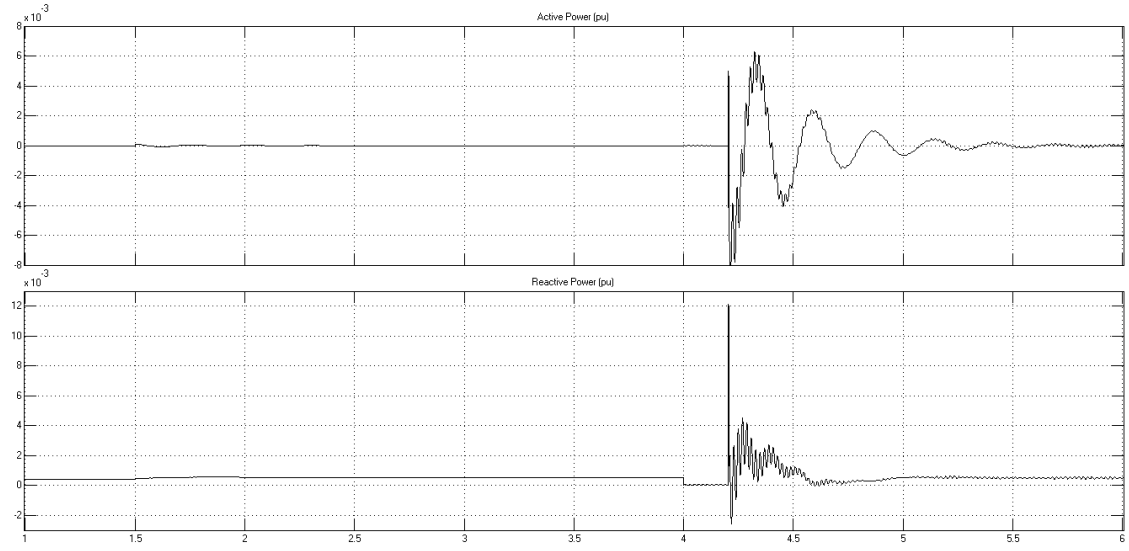

Figure 6.3: Active and Reactive Power for AVR case. [X-axis: 0.5 s/div.; Y-axis: 0.002 pu/div.]

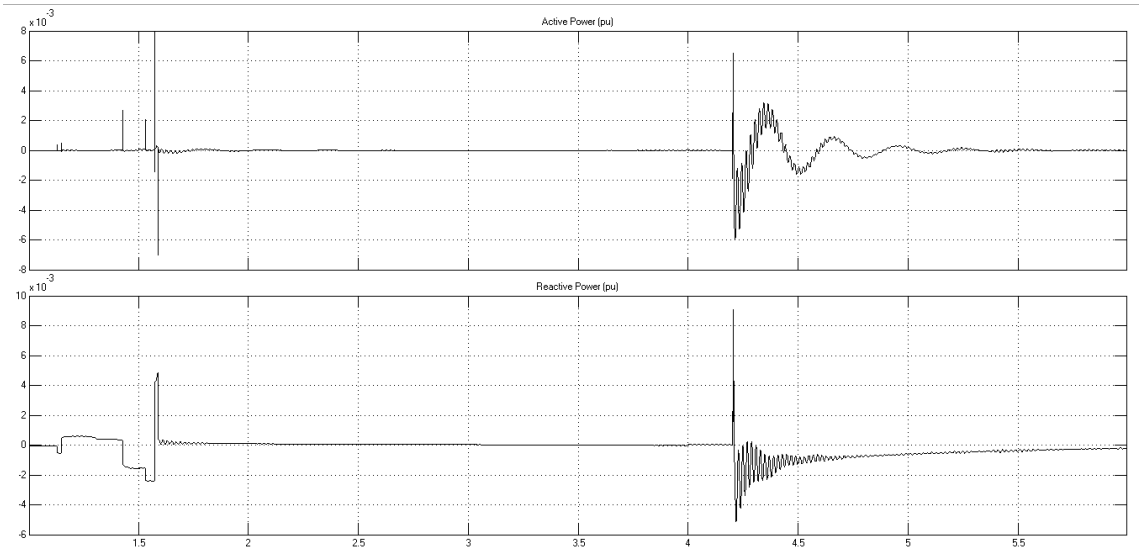

Figure 6.4: Active and Reactive Power with IDA-PBC. [X-axis: 0.5 s/div.; Y-axis: 0.002 pu/div.]

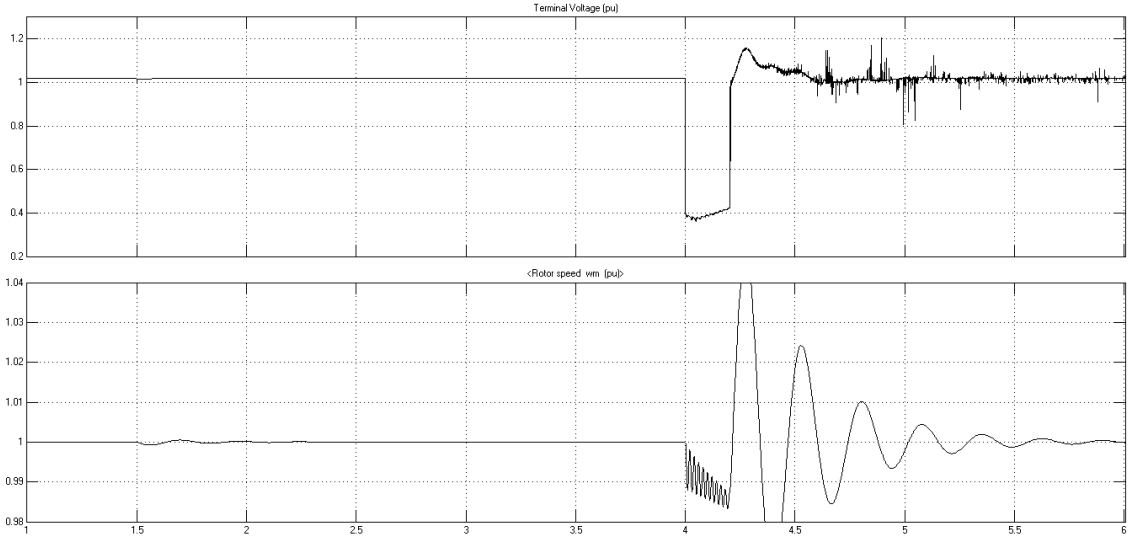

Figure 6.5: Terminal Voltage and Rotor Speed with AVR. [X-axis: 0.5 s/div.; Y-axis: Plot1: 0.2 pu/div., Plot2: 0.01 pu/div.]

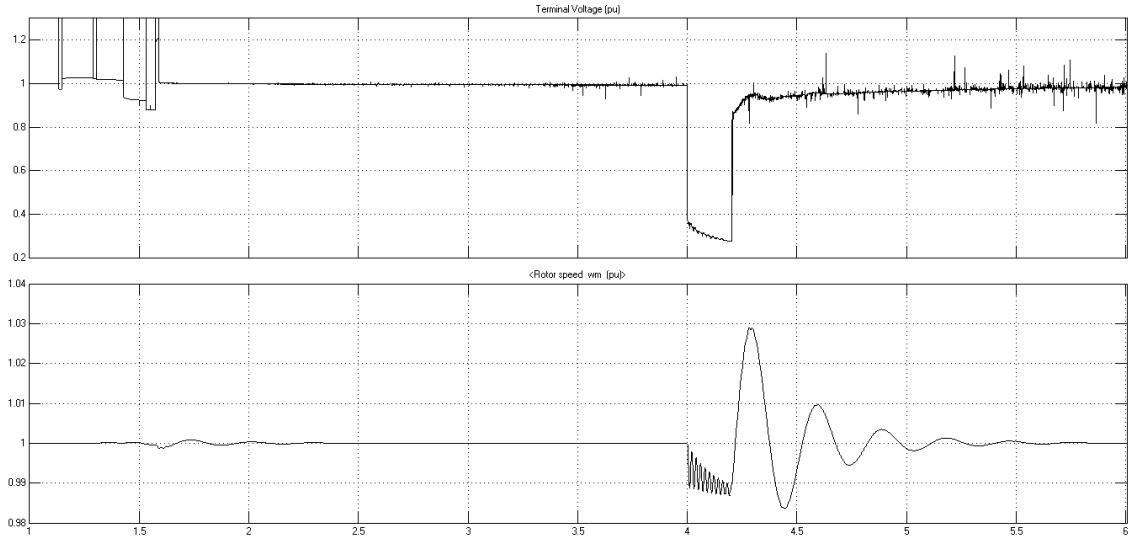

Figure 6.6: Terminal Voltage and Rotor speed with IDA-PBC. [X-axis: 0.5 s/div.; Y-axis: Plot1: 0.2 pu/div., Plot2: 0.01 pu/div.]

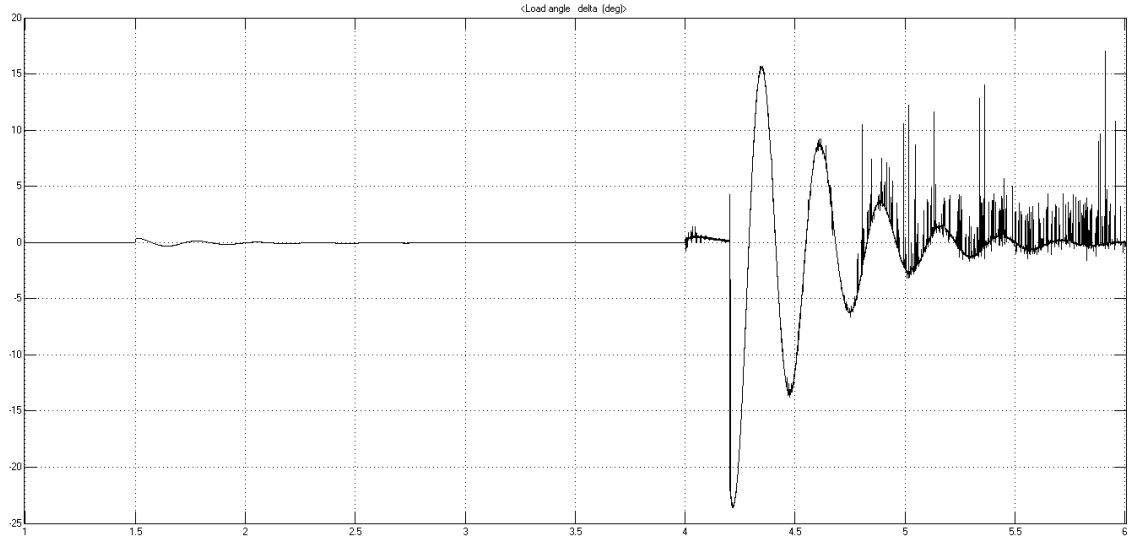

Figure 6.7: Load Angle with AVR. [X-axis: 0.5 s/div.; Y-axis: 5 degrees/div.]

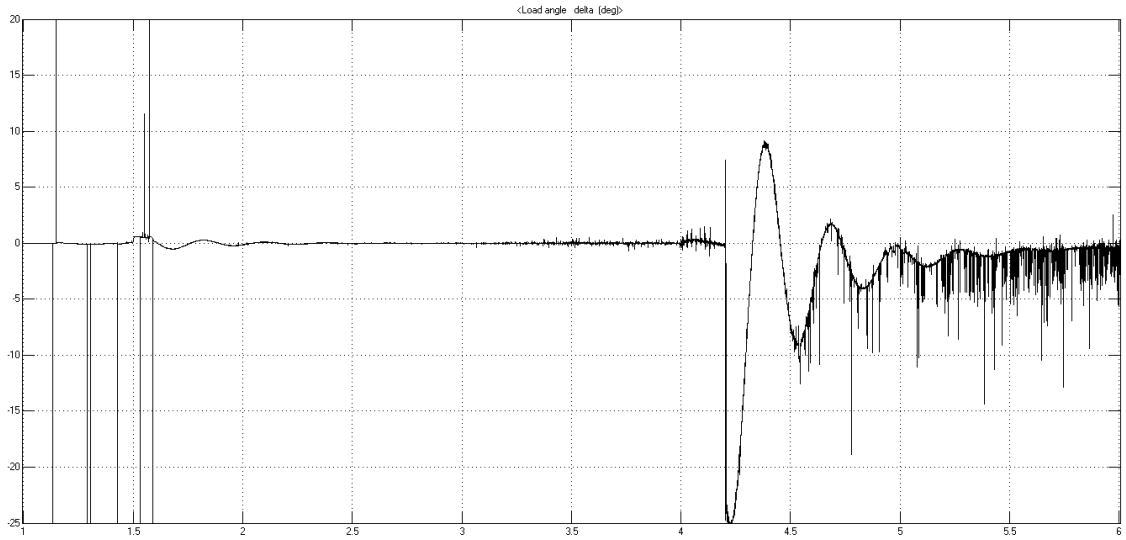

Figure 6.8: Load Angle Power with IDA-PBC. [X-axis: 0.5 s/div.; Y-axis: 5 degrees/div.]

Chapter 7

Reduction of Signal requirement

All the control algorithms for generator excitation controller require certain minimum amount of signals that needs to be measured instantaneously and then only the required output can be obtained. The signals that are generally required are listed below:

1. Three line voltages (3)
2. Three line currents (3)
3. Load angle (1)
4. Rotor mechanical speed (1)
5. Active and Reactive power (2)
6. Power factor (1)

As it can be seen that there are total eleven signals and all the algorithms require most of them. In order to have excitation system economically viable, measuring each of the signals cannot be afforded. Also, since complexity increases, the reliability, fault escalation and controller requirements also increases making the task difficult to mitigate. Some of the signal measurements may not be required since they can be estimated. For example, power factor can be obtained if active power and reactive power can be measured. Hence only ten signals remain that can be given to controller as an input.
It is known that active power and reactive power can be obtained with the help of line currents and voltages. Hence this again results in reduction of signals by two. If active and reactive powers can be estimated correctly then load angle can be calculated easily that eliminates one more signal input. Hence the number of signal requirements remain seven and they are:

1. Three line voltages (3)

2. Three line currents (3)

3. Rotor mechanical speed (1)

The speed measurement is generally not preferable because of the economical and reliability purposes. Hence it becomes a necessity to eliminate it resulting in reduction of number of signals to six.

7.1 State Estimation of Active and Reactive Powers

It is assumed that three line voltages and three line currents i.e. V_{ab}, V_{bc}, V_{ca}, I_a, I_b and I_c are the only measurements that are obtained from measuring instruments. Hence active power (P) and reactive power (Q) can be evaluated from the following equations:

$$P = V_{ab}.I_a - V_{bc}.I_c \tag{7.1}$$

$$Q = [V_{ab}.I_c + V_{bc}.I_a + V_{ca}.I_b]/\sqrt{3} \tag{7.2}$$

$$\delta = \arctan \frac{I.X_q.P - I.R.Q}{V.S + I.X_q.Q + I.R.P} \tag{7.3}$$

where **I** and **V** are any of the instantaneous line currents and voltages. **R** and X_q are the armature resistance and reactance of the synchronous generator. **S** is the apparent power which can be obtained from

$$S = \sqrt{P^2 + Q^2} \tag{7.4}$$

Under balanced conditions

$$V_{ab} + V_{bc} + V_{ca} = 0 \tag{7.5}$$

$$I_a + I_b + I_c = 0 \tag{7.6}$$

Hence the reactive power can be rewritten as

$$Q = V_{ab}.I_c + V_{bc}.I_a + (V_{ab} + V_{bc}).(I_a + I_c)]/\sqrt{3} \tag{7.7}$$

$$Q = [V_{ab}.(2I_c + I_a) + V_{bc}.(2I_a + I_c)]/\sqrt{3} \tag{7.8}$$

Thus it can be observed that for obtaining P and Q both, only four measurements i.e. two line voltages and two line currents are required and hence giving a redundancy factor of 2. If six measurements are used for the estimation of these two state variables, it would give the redundancy factor of 3 which is generally not preferred.
From equation 7.1 and 7.8 we can write

$$\begin{bmatrix} P \\ Q \end{bmatrix} = \begin{bmatrix} I_a & -I_c \\ (2I_c + I_a)/\sqrt{3} & (2I_a + I_c)/\sqrt{3} \end{bmatrix} \begin{bmatrix} V_{ab} \\ V_{bc} \end{bmatrix} \tag{7.9}$$

Hence

$$\begin{bmatrix} V_{ab} \\ V_{bc} \end{bmatrix} = \frac{1}{A} \begin{bmatrix} (2I_a + I_c)/\sqrt{3} & I_c \\ -(2I_c + I_a)/\sqrt{3} & I_a \end{bmatrix} \begin{bmatrix} P \\ Q \end{bmatrix}$$

where

$$A = 2(I_a^2 + I_c^2 + I_a.I_c)/\sqrt{3} \tag{7.11}$$

Rewriting equation 7.7,

$$Q = [I_a(2V_{bc} + V_{ab}) + I_c(2V_{ab} + V_{bc})]/\sqrt{3} \tag{7.12}$$

Hence following the same procedure it can be obtained that

$$\begin{bmatrix} I_a \\ I_c \end{bmatrix} = \frac{1}{B} \begin{bmatrix} (2V_{bc} + V_{ab})/\sqrt{3} & V_{bc} \\ -(2V_{ab} + V_{bc})/\sqrt{3} & V_{ab} \end{bmatrix} \begin{bmatrix} P \\ Q \end{bmatrix}$$

where

$$B = 2(V_{ab}^2 + V_{bc}^2 + V_{ab}.V_{bc})/\sqrt{3} \tag{7.14}$$

From these equations, the functions of measurements in terms of state variables are obtained that are needed for estimation.

Hence from equation and matrix of 7.11 and 7.14:

$$f_1(P,Q) = \frac{1}{A}.[P\frac{(2I_a + I_c)}{\sqrt{3}} + Q.I_c] \tag{7.15}$$

$$f_2(P,Q) = \frac{1}{A}.[-P\frac{(2I_c + I_a)}{\sqrt{3}} + Q.I_a] \tag{7.16}$$

$$f_3(P,Q) = \frac{1}{B}.[P\frac{(2V_{ab} + V_{bc})}{\sqrt{3}} + Q.V_{bc}] \tag{7.17}$$

$$f_4(P,Q) = \frac{1}{B}.[-P\frac{(2V_{bc} + V_{ab})}{\sqrt{3}} + Q.V_{ab}] \tag{7.18}$$

We can define the weighted matrix W as

$$W = \begin{bmatrix} \frac{1}{\sigma_1^2} & 0 & 0 & 0 \\ 0 & \frac{1}{\sigma_2^2} & 0 & 0 \\ 0 & 0 & \frac{1}{\sigma_3^2} & 0 \\ 0 & 0 & 0 & \frac{1}{\sigma_4^2} \end{bmatrix} \tag{7.19}$$

where σ_1, σ_2, σ_3 and σ_4 are the standard deviations of the measurements V_{ab}, V_{bc}, I_a and I_c respectively. The coefficient matrix H is given by

$$H = \begin{bmatrix} (2I_a + I_c)/(A\sqrt{3}) & I_c/A \\ -(2I_a + I_c)/(A\sqrt{3}) & I_a/A \\ (2V_{ab} + V_{bc})/(B\sqrt{3}) & V_{bc}/B \\ -(2V_{bc} + V_{ab})/(B\sqrt{3}) & V_{ab}/B \end{bmatrix} \tag{7.20}$$

The estimation can be obtained as

$$x^{est} = [H^T W H]^{-1} H^T W z^{meas} \tag{7.21}$$

where $x^{est} = \begin{bmatrix} P \\ Q \end{bmatrix}$, $z^{meas} = \begin{bmatrix} V_{ab} \\ V_{bc} \\ I_a \\ I_c \end{bmatrix}$

Hence it can be concluded that active and reactive power both can be estimated by simply using four measurements according to equations 7.21. Further the load angle δ can also be measured using equation 7.3. The only variable that needs to be estimated now is rotor speed ω which is discussed in the following section.

7.2 Load Angle δ Estimation

Since active and reactive power are estimated in the previous section, load angle δ can be calculated from equation 7.3. The estimation of load angle is shown below considering P and Q as constant and measurements required are one line voltage **V** and one line current **I**. Let **C** be defined such that:

$$C = tan(\delta) \tag{7.22}$$

Therefore

$$C = \frac{I.X_q.P - I.R.Q}{V.S + I.X_q.Q + I.R.P} \tag{7.23}$$

$$V.S.C + I.X_q.Q.C + I.R.P.C = I.X_q.P - I.R.Q \tag{7.24}$$

Hence we can obtain

$$I = \frac{-V.S.C}{X_q.Q.C + R.P.C - P.X_q + R.Q} \tag{7.25}$$

$$I = \frac{V.S.C}{P.X_q - R.Q}.\left[1 - \frac{X_q.Q.C + R.P.C}{P.X_q - R.Q}\right]^{-1} \tag{7.26}$$

Using series expansion at point C_o and then solving we get

$$I = \frac{V.S.C}{(P.X_q - R.Q)^2}.[(P.X_q - R.Q)C_o + (X_q.Q + R.P).(C - C_o)^2] \tag{7.27}$$

If C_o is taken near C then $C - C_o$ is very less and hence $(C - C_o)^2$ can be neglected. Hence we can obtain

$$I = \frac{V.S.C.C_o}{P.X_q - R.Q} \tag{7.28}$$

Again from equation 7.24, it can be obtained that

$$V = I\frac{(P.X_q - R.Q)}{S.C} - I(Q.X_q - R.P) \tag{7.29}$$

Again taking the Taylor series expansion at point C_o, equation 7.29 can be obtained as

$$V = -I(Q.X_q - R.P) + (P.X_q - R.Q).\left[\frac{1}{C_o} - \frac{C-C_o}{C_o^2}\right] \tag{7.30}$$

Following the same procedure as was followed for estimation of active and reactive power, the coefficient matrix for this case $\mathbf{H}_1 can be obtained as$

$$H_1 = \begin{bmatrix} V.S.C_o/(P.X_q - R.Q \\ I(R.Q - P.X_q)/C_o^2 \end{bmatrix} \tag{7.31}$$

Thus the estimation of C i.e. tan δ can be obtained as

$$C = (H_1^T.W.H_1)^{-1}.H_1^T.W.H_1.z^{meas} \tag{7.32}$$

where z^{meas}=[I V]^T and W= diag[$1/\sigma_1^2$, $1/\sigma_2^2$]. σ_1 and σ_2 are the standard deviation of the instruments measuring the current and voltage respectively.
These equations are valid only when

$$C < \frac{P.X - R.Q}{X.Q + R.P} \tag{7.33}$$

In order to obtain δ for the range where eq. 7.33 is not satisfied, one more parameter D is defined similarly as before i.e.

$$D = cot(\delta) \tag{7.34}$$

$$D = \frac{V.S + I.X_q + I.R.P}{I.X_q.P - I.R.Q} \tag{7.35}$$

Thus following the similar procedure as before the equations after taylor series expansion can be obtained as

$$I = \frac{-V.S}{(Q.X_q. + R.P)^2}.[Q.X_q. + R.P + D(P.X_q. - R.Q)] \tag{7.36}$$

$$V = \frac{(X_q.P.I - R.Q.I)(D - D_o) - X_Q.Q.I - R.P.I}{S} \tag{7.37}$$

D_o is the initial value. Hence the coefficient matrix is

$$H_2 = \begin{bmatrix} V.S(R.Q - X_q.P)/(X_q.Q + R.P)^2 \\ (X_q.P.I - R.Q.I)/S \end{bmatrix}$$

Thus D can be estimated as

$$D = (H_2^T.W.H_2)^{-1}.H_2^T.W.H_2.z^{meas} \tag{7.39}$$

$$D < \frac{X.Q + R.P}{P.X - RQ} \tag{7.40}$$

where z^{meas}=[I V]^T and W= diag[$1/\sigma_1^2$, $1/\sigma_2^2$]. σ_1 and σ_2 are the standard deviation of the instruments measuring the current and voltage respectively.
Thus δ can be estimated.

7.3 Rotor Speed Estimation

There are many instruments available to measure the speed and these signals can be given to the controller. But these add up to the total cost and hence reliability is compromised. Hence it is much more preferable to avoid these signals and be calculated or estimated within the controller. In order to obtain it, frequency of the system and the frequency of oscillations of rotor needs to be determined. Since in the SMIB case, the grid frequency remains constant, the frequency of oscillations of rotor is only needed to be determined. When load gets changed, the rotor starts oscillating around the synchronous speed due to the imbalance between the mechanical power and electrical power. Hence the oscillations in the active power can be observed. This frequency can be determined by the flowchart of figure 7.1.

It can be observed that the power is measured or estimated first in flowchart of figure 7.1. The instantaneous reading is subtracted from previous reading and accordingly a gain is multiplied. Thus power oscillations are obtained around zero axis in measurable form. After then it is checked that whether power oscillation is crossing the zero axis and accordingly time is noted down for both instants i.e. when it enters positive half cycle from negative half cycle and vice-versa. The difference of both these corresponding times are taken and after inverting this time difference, rotor frequency oscillations are obtained.

In figure 7.2 the estimated and the measured variables are shown. It can be observed that active and reactive power matches exactly at each instant of time and hence they are overlapped, while there is certain error observed in load angle estimation. But the results obtained after applying the derivative of both estimated and measured load angles shows that derivative of estimated load angle follows the same pattern as of the rotor oscillations around the synchronous speed.

In figure 7.3, the active power and rotor oscillations are observed. It can be seen that the derivative of the load angle do not follow the rotor oscillations exactly especially during the initial period. Hence the power oscillations are obtained according to the flowchart discussed before and hence almost the same behaviour is observed as that of rotor oscillations. Thus, the change in speed can be obtained easily from the programming.

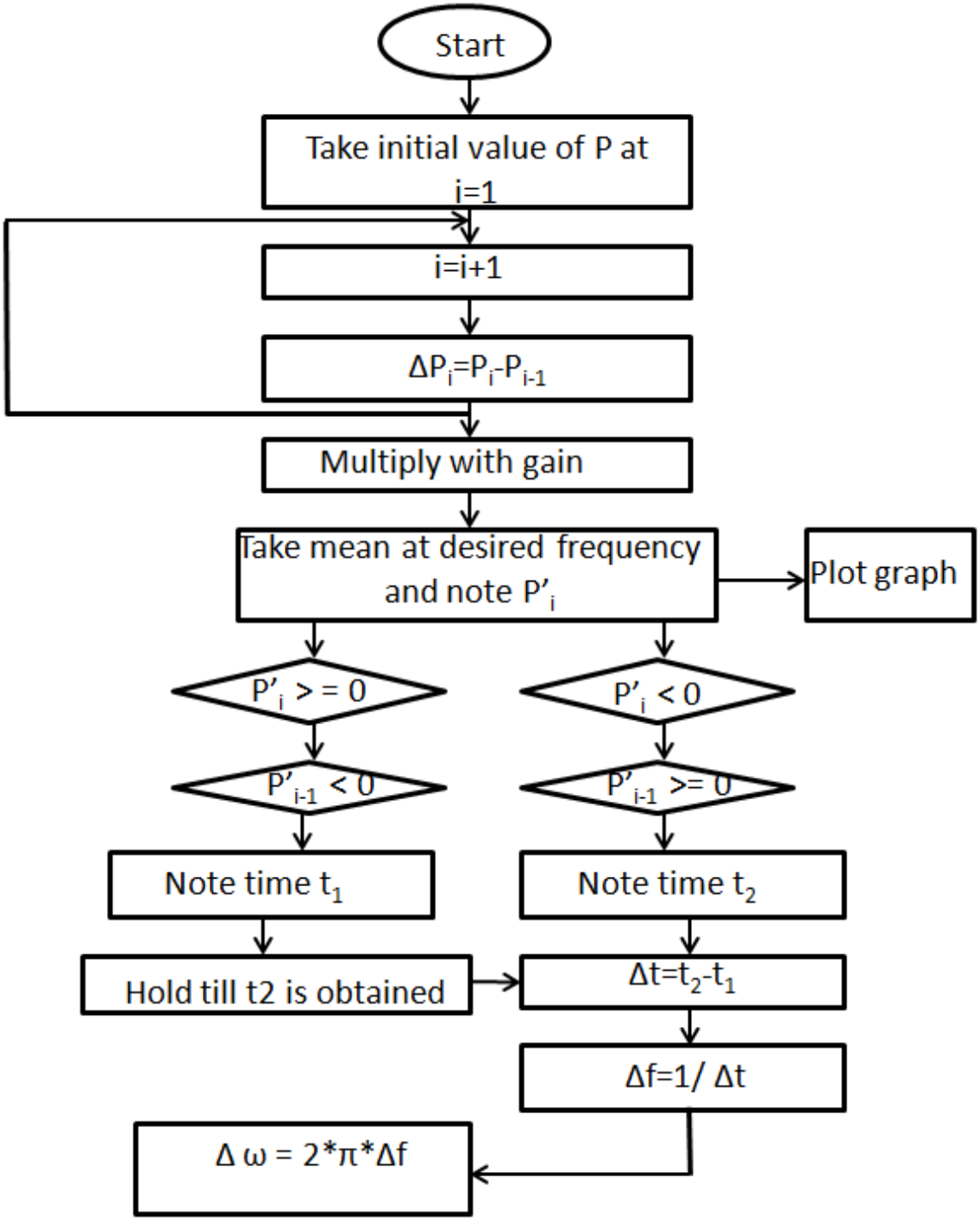

Figure 7.1: Flowchart for rotor oscillation frequency

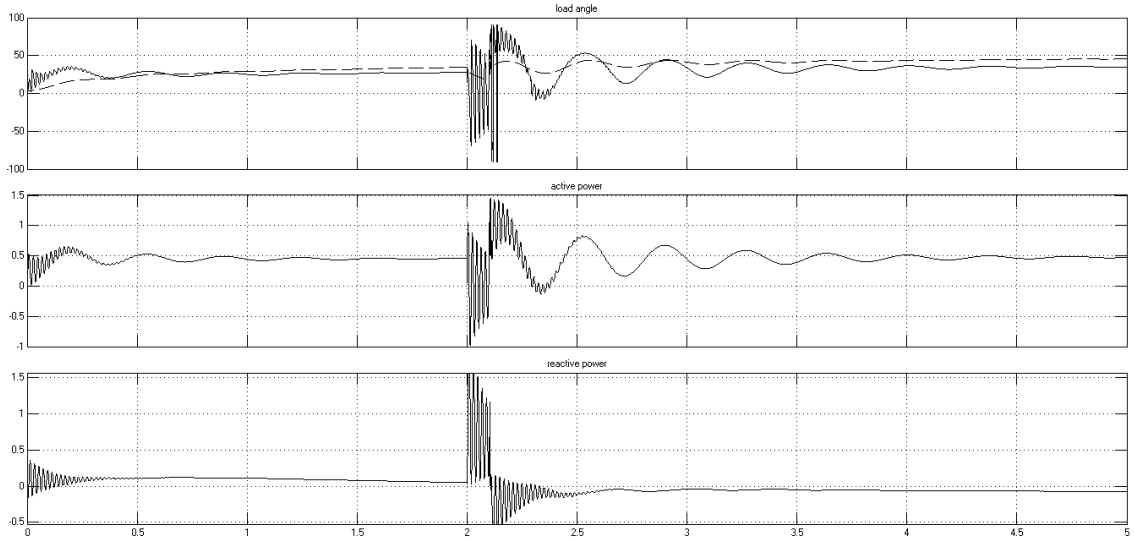

Figure 7.2: Estimated and Measured variables. [X-axis: 0.5 s/div.; Y-axis: Plot1: 50 degree/div., Plot2: 0.5 pu/div., Plot3: 0.5 pu/div.]

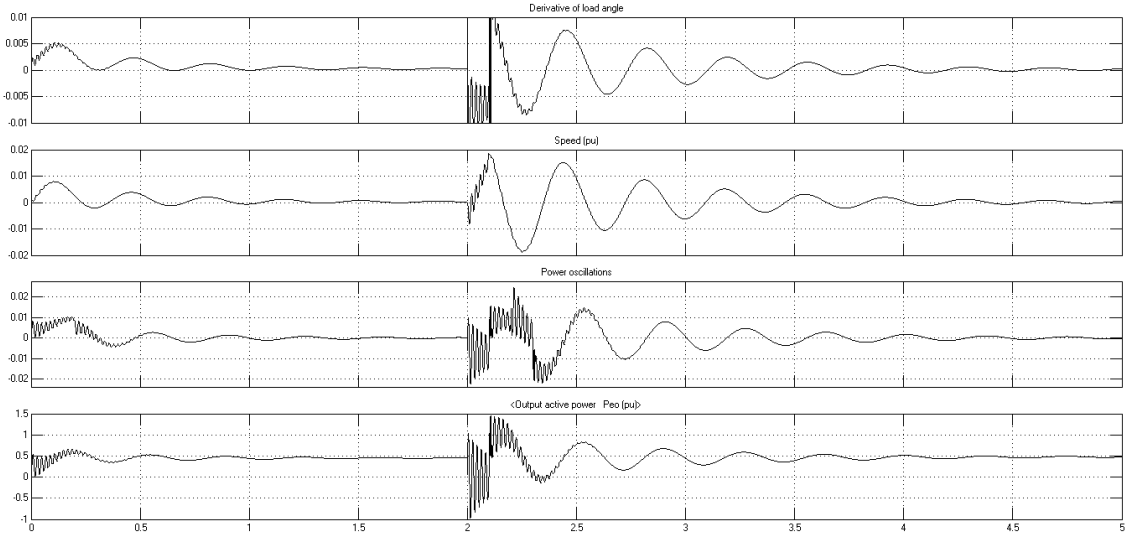

Figure 7.3: Rotor and Power oscillations. [X-axis: 0.5 s/div.; Y-axis: Plot1: 0.005 rad/div., Plot2: 0.01 pu/div., Plot3: 0.01 pu/div., Plot4: 0.5 pu/div.]

Chapter 8

Implementation of AVR and PSS

8.1 Implementation of Automatic Voltage Regulators (AVR) only

From [8], the torque coefficient in Laplace domain can be obtained as

$$\frac{[\Delta T_e]_{\Delta E'_q}}{\Delta\delta} = \frac{-K_2K_3[K_4(1+sT_R)+K_5K_A]}{(K_3T'_{do}T_R)s^2+(K_3T'_{do}+T_R)s+(1+K_3K_6K_A)} \tag{8.1}$$

Thus we can obtain

$$\frac{[\Delta T_e]_{\Delta E'_q}}{\Delta\delta} = \frac{-K_2K_3[(1+jwT_R)K_4+K_5K_A]}{1+K_3K_6K_A-K_3T'_{do}T_Rw^2+j(K_3T'_{do}+T_R)w} \tag{8.2}$$

where w is frequency of oscillations. The damping torque coefficient $[K_D]_{AVR}$ can be obtained as

$$[K_D]_{AVR} = \frac{-K_2K_3[(1+K_3K_6K_A-K_3T'_{do}T_Rw^2)K_4T_Rw-(K_4+K_5K_A)(K_3T'_{do}+T_R)w]}{(1+K_3K_6K_A-K_3T'_{do}T_Rw^2)^2+(K_3T'_{do}+T_R)^2w^2} \tag{8.3}$$

Applying Routh-Hurwitz criterion on equation 8.1 we can obtain that

$$K_A > \frac{-1}{K_3K_6} \tag{8.4}$$

for system to be stable. Also $(K_4 + K_5K_A) > 0$ i.e. $K_A > (-K_4/K_5)$ to mitigate the demagnetization effect. Again from characteristic equation of eq 8.1 it can be obtained that

$$K_A = \frac{1}{K_3K_6}[\frac{(K_3T'_{do} + T_R)^2}{4K_3T'_{do}T_R} - 1] \tag{8.5}$$

Since the value of AVR gain i.e. K_A is high, hence the system remains stable as long as K_5 is positive. If K_5 is negative then the product K_5K_A is very high and hence the damping torque coefficient becomes negative from eq. 8.3, thus making the system unstable. In order to mitigate this problem, Power System Stabilizers are implemented.

8.2 Implementation of Power System Stabilizers (PSS)

From [8], considering $T_R = 0$, the transfer function for torque coefficient after implementation of PSS for very small changes in δ is given by

$$\frac{[\Delta T_e]_{\Delta X_2}}{\Delta X_s} = \frac{K_2K_3K_A}{1 + K_3K_6K_A + K_3T'_{do}s} \tag{8.6}$$

The magnitude M and angle α can be obtained in terms of frequency of oscillations as

$$M = \frac{K_2K_3K_A}{[(1 + K_3K_6K_A)^2 + (K_3T'_{do}w)^2]^{1/2}} \tag{8.7}$$

$$\alpha = -arctangent\frac{-K_3T'_{do}w}{1 + K_3K_6K_A} \tag{8.8}$$

If the damping coefficient due to PSS is $[K_D]_{PSS}$, then the net damping coefficient $[K_D]_{net}$ can be given by

$$[K_D]_{net} = [K_D]_{AVR} + [K_D]_{PSS} \tag{8.9}$$

Thus in order to have a net positive damping coefficient,

$$[K_D]_{PSS} > -[K_D]_{AVR} \tag{8.10}$$

Hence

$$G_{PSS}\frac{K_2K_3K_A}{[(1+K_3K_6K_A)^2+(K_3T'_{do}w)^2]^{1/2}} > \frac{K_2K_3^2T'_{do}(K_4+K_5K_A)w}{(1+K_3K_6K_A)^2+(K_3T'_{do}w)^2} \tag{8.11}$$

If K_{pss} is the gain of PSS then it can be obtained from the equation 8.11

$$K_{pss} > \frac{K_3T'_{do}(K_4+K_5K_A)w}{K_A[(1+K_3K_6K_A)^2+(K_3T'_{do}w)^2]^{1/2}} \tag{8.12}$$

Thus the gain can be obtained from the above equation and the angle of lag compensation can be obtained as from equation 8.8 for which the time constant T_1 and T_2 for a lag compensator $\frac{1+sT_1}{1+sT_2}$ should follow the following relations.

$$\frac{K_3T'_{do}}{1+K_3K_6K_A} = \frac{T_1-T_2}{1+w^2T_1T_2} \tag{8.13}$$

The ratio of T_1 and T_2 can be taken as 10. But it can also be determined specifically for a system as explained by [9].

8.3 Flowchart

Figure 8.1 shows the flowchart for the implementation of AVRs and PSS both. Firstly, the gain of the AVRs i.e. K_A can be obtained considering the various conditions obtained in section 8.1. Approximately it can be calculated as:

$$K_A = \frac{T'_{do}}{4T_R} \tag{8.14}$$

where T_R is the transducer time constant and is taken equal to 0.01 seconds.
After this for various iterations, line voltages and line currents are taken as inputs and active as well as reactive powers are estimated as it was discussed in chapter 6. After the estimation DQ0 transformation of line voltages and line currents and

hence δ is calculated. It can also be estimated as was discussed in chapter in 6, but in order to reduce the manipulations it is directly calculated at this stage. if it changes significantly, say 1 degree, then heffron phillips constants K_3 to K_6 are calculated. All these estimated data are stored and used to calculate the oscillation frequency. If it lies within the small signal range then accordingly gain of the PSS and time constant for lag compensation is calculated from equation 8.12 and 8.13 respectively, so the signal V_P can be given further by equation 8.14. If not then V_P is taken as zero.

$$V_p = K_{pss}\frac{(1+sT_1)}{(1+sT_2)}\frac{sT_w}{(1+sT_w)} \tag{8.15}$$

where T_w can be taken between 1 to 20 seconds.
After this the output signal or field voltage can be given by equation 8.15.

$$V_f = K_A(V_t - V_{ref} + V_p) \tag{8.16}$$

where V_t is the terminal voltage.

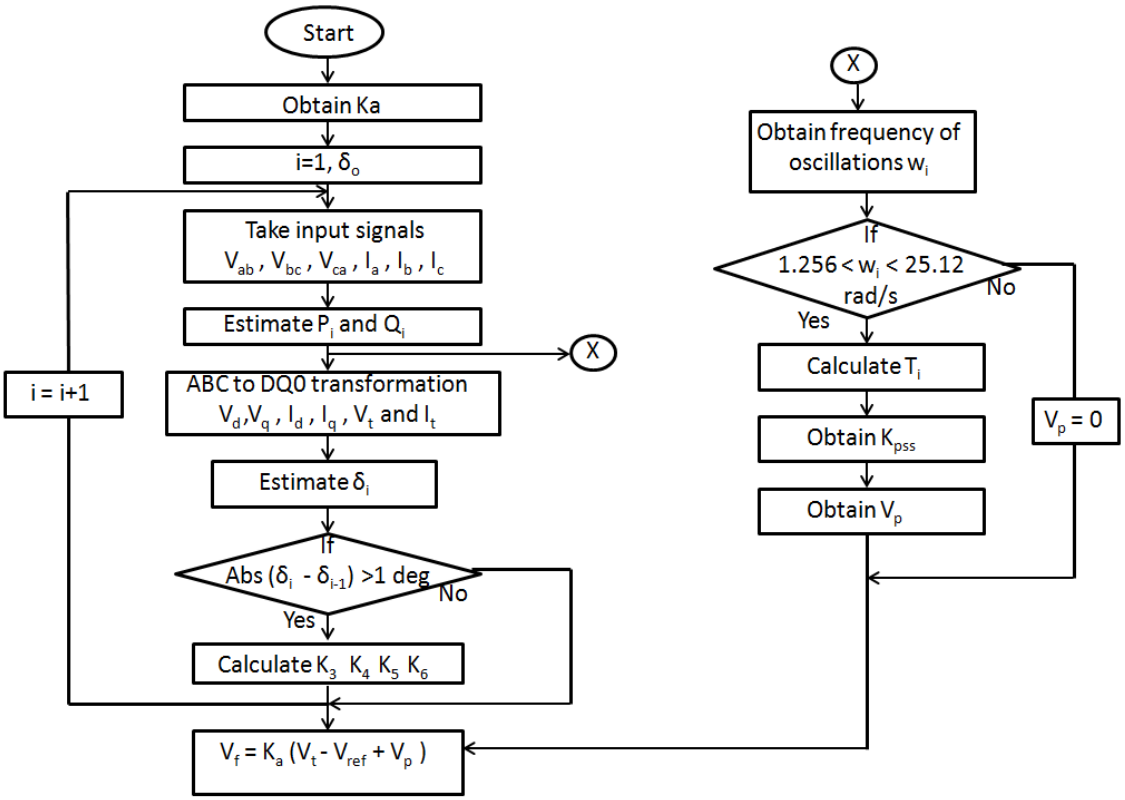

Figure 8.1: Flowchart for AVR+PSS implementation

Chapter 9

Hardware Implementation

It is evident that all the control algorithms for generator excitation controller irrespective of the approach used creates the excitation response in form of excitation voltage. According to this response the firing pulses are created and are given to the gate of power electronic switches of exciters and hence the output voltage is provided to the field winding of the synchronous generator. Thus the hardware implementation was done in two parts. (1) Generation of firing pulses and excitation output voltage signal and (2) Response of fully controlled thyristor Rectifier.

9.1 Generation of firing pulses and excitation output voltage signal ($\mathbf{E}_{fd}$)

For generating the firing pulses, DSpace package was used. The control part from the MATLAB simulation was only kept to generate *.sdf* file which is required by DSpace for the creation of Project. The *slider* was used to vary the Reference voltage and terminal voltage and accordingly the responses were generated which were observed on *plotter* on DSpace as well as on Digital Signal Oscilloscope .
Figure 9.1 shows the MATLAB simulation for generating the firing pulses in DSpace. It can be observed that the simulation can be categorized in two parts:

9.1.1 Generation of $\mathbf{E}_{fd}$

Generation of E_{fd} voltage signal by comparing the reference voltage V_{ref} and Terminal Voltage V_t which is then passed through the AVR gain. Since the gain of AVR is generally high, if there is a large difference between V_t and V_{ref} then E_{fd} will be much higher. Generally, the upper limit of E_{fd} is kept between 2.5 pu to 14 pu according to the field forcing capability. According to [4] the field forcing capability should be twice that of the rated field current I_{fd}. In order to limit E_{fd} within this range, limiters are provided as can be observed from the simulation.

9.1.2 Generation of firing pulses

After the generation of E_{fd} signal, it is passed through a *subtract* block, where the value of the signal is subtracted from the highest limit of E_{fd} to be permitted. this new value is then compared with the sinusoidal signal of respective phase which can be obtained easily. Either all the three AC voltage inputs of the thyristor can be obtained as signals or any one phase signal can be obtained and the rest of the phases can be provided a 120 degree phase shift. The signals should be such that the peak of the sine wave is little (maybe 1%) higher than the E_{fd} upper limit. When the value of sine wave is higher than this DC value i.e. the subrtracted E_{fd} value, pulse is generated for that respective thyristor according to the phase. Thus in this way firing pulses for thyristor switches T_1, T_3 and T_5 can be generated taking their respective phase sine waves. For generating the pulses for switches T_4, T_6 and T_2, the same comparison can be done but the subtracted E_{fd} value is inverted. Thus the firing pulses are generated.

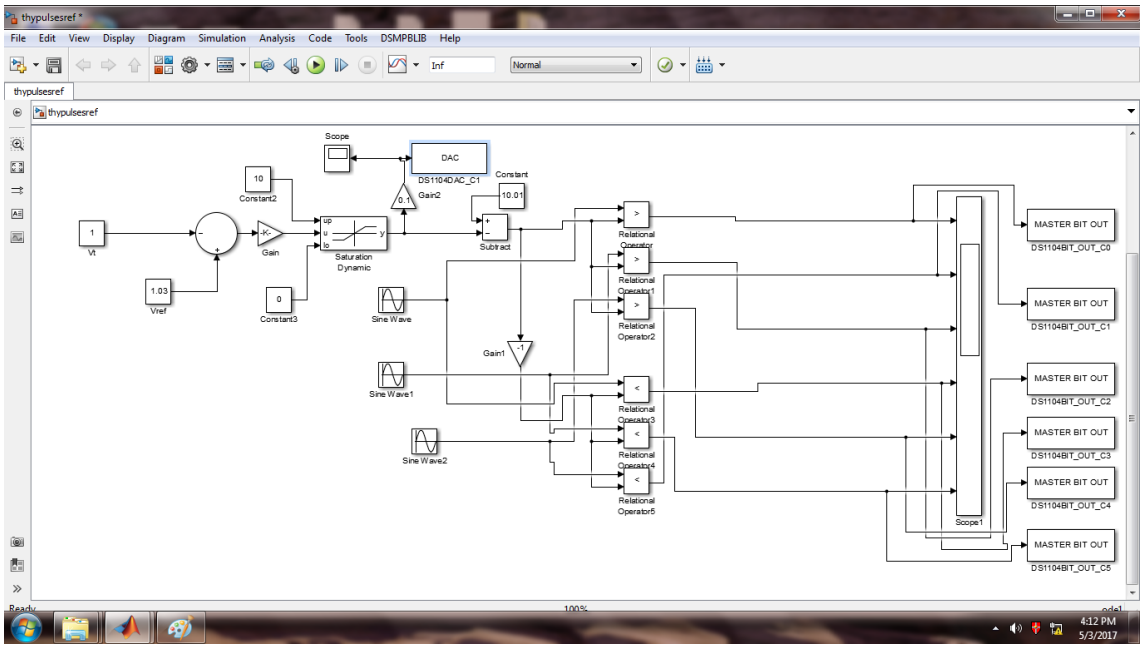

Figure 9.1: MATLAB Simulation for E_{fd} and Firing Pulses

Figure 9.2 shows the response or change in firing pulses according to the change in terminal voltage. The terminal voltage is changed using the repeating sequence block. It can be observed that initially the terminal voltage is 0.95 pu and the reference voltage is kept constant at 1.03 pu. It increases to 1 pu till time 0.1 s. after that the terminal voltage increases to 1.04 pu till time 0.5 s and then reduced. It can be observed that as terminal voltage moves closer towards the reference voltage the firing pulse gets reduced. When it goes above the reference voltage the firing pulse becomes zero and hence no field voltage will be applied. As soon as the terminal voltage gets reduced to a value lesser than reference voltage, firing pulse is

again generated and increases further as terminal voltage is reduced. Thus a desired response is obtained. This firing pulse can be applied to thyristor bridge rectifier as well as IGBT based bridge rectifier.

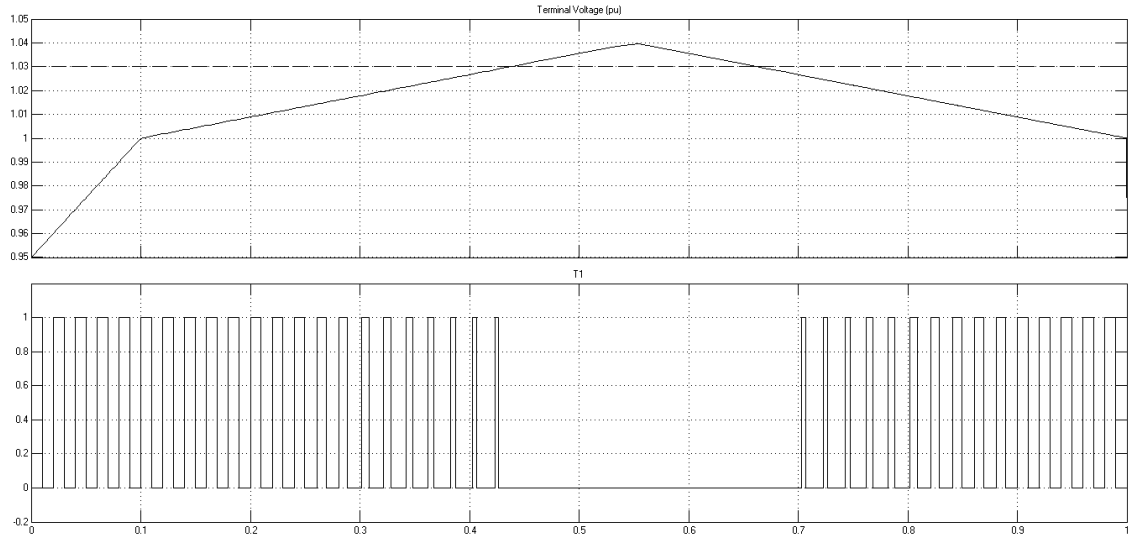

Figure 9.2: Simulation Result for E_{fd} and Firing Pulses. [X-axis: 0.1 s/div.; Y-axis: Plot1: 0.01 pu/div, Plot2: 0.2 pu/div.]

After the creation of MATLAB model is *build* resulting into the creation of *.sdf* file which is utilized in DSpace for the creation of project. Figure 9.3 shows the DSpace window where the *plotter* is showing the pulses for one of the thyristor switch and E_{fd} during online mode. The V_t and V_{ref} can be changed using the *slider*. The pulses are then taken on the output channel through Digital I/O ports while E_{fd} signal is obtained through DAC channel since it is an analog signal ranging between 0 to 10 volts. Thus the signals are seen on the Digital Signal Oscilloscope. Figure 9.4 shows the of DSpace i.e. E_{fd} and firing pulses for T_1 on Digital Signal Oscilloscope. It consist of two cases. In first case i.e. fig 9.4a, the terminal voltage is decreased continuously from the DSpace window so that E_{fd} increases continuously since it is dependent on the difference between reference voltage and terminal voltage. Since E_{fd} is rising continuously, it depicts that firing pulses should be increased to move the rectifier towards the higher output voltage. Hence firing pulses will start generating and their pulse width will increase continuously till the field forcing is achieved. Similarly, vice versa happens in other case i.e. 9.4b.

Figure 9.5 shows the firing pulses for switches T_1 to T_6 for $V_t = 0.97$ pu and $V_{ref} = 1.05$ pu. Fig. 9.5a shows pulses for T_1, T_2, T_3 and T_4 having the phase difference of 60 degree between each other. Fig. 9.5b shows two pair of switches i.e. T_1, T_4 and T_3, T_5. Similarly the fig. 9.5c and 9.5d shows the pulses for switches of upper and lower half of rectifier bridge respectively.
Figure 9.6 shows the firing pulses for switches T_1 and T_4 only but for different values

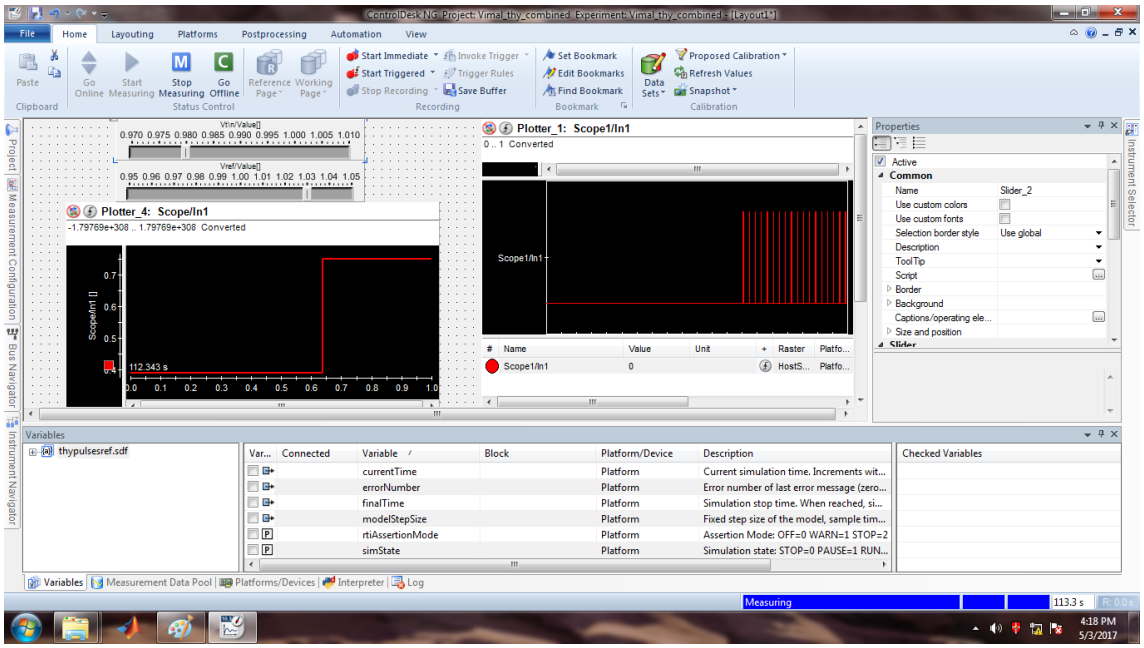

Figure 9.3: DSpace Simulation

of terminal voltage V_t and reference voltage V_{ref}. Hence accordingly the change in pulse width can be observed.

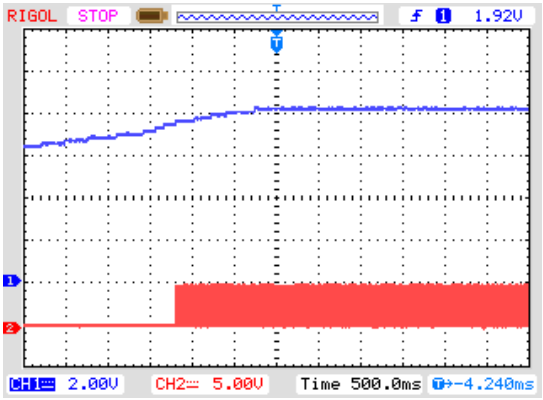

(a) Increasing V_t

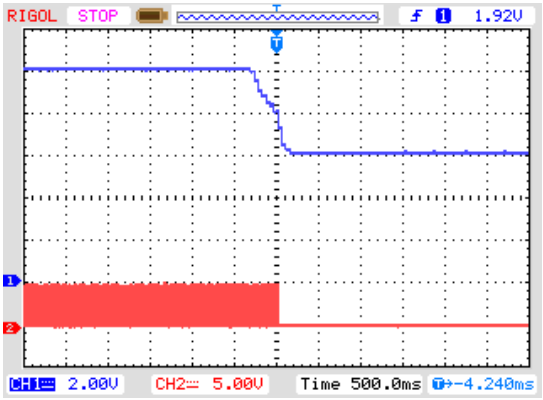

(b) Decreasing V_t

Figure 9.4: Response of changing V_t on firing pulses

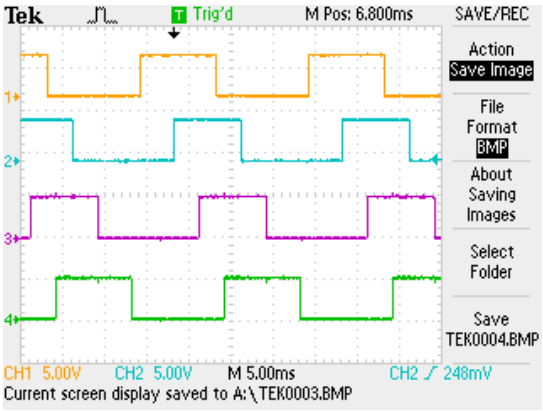

(a) T_1, T_2, T_3 and T_4

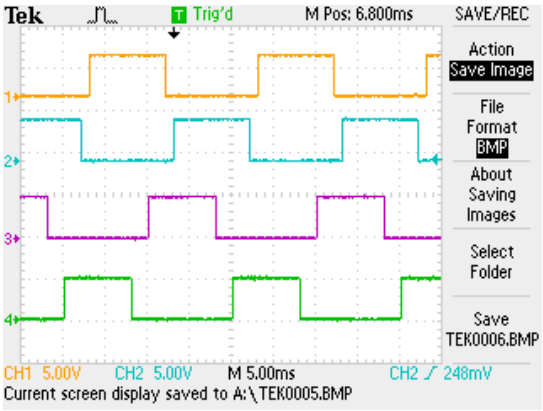

(b) T_1, T_4 and T_3, T_6

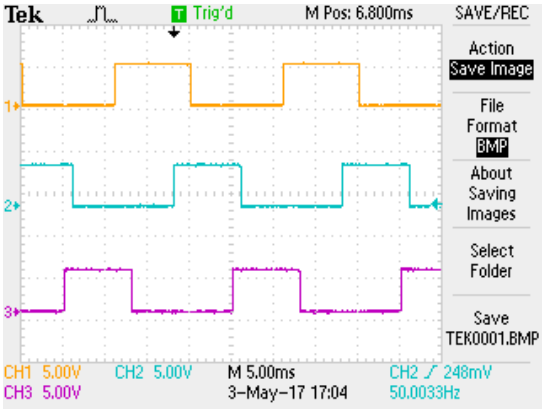

(c) T_1, T_3 and T_5

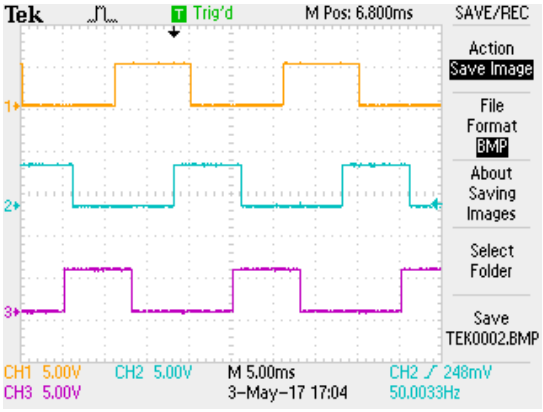

(d) T_4, T_6 and T_2

Figure 9.5: Firing Pulses for Thyristor Switches

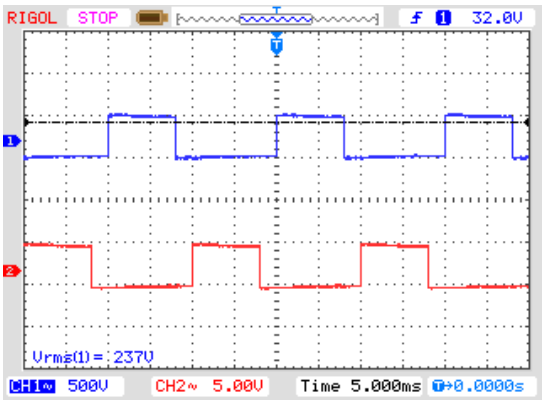

(a) $V_t = 0.99$ pu, $V_{ref} = 1.05$ pu

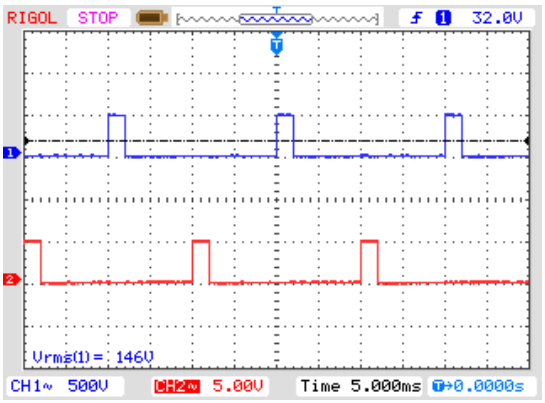

(b) $V_t = 1$ pu, $V_{ref} = 1.05$ pu

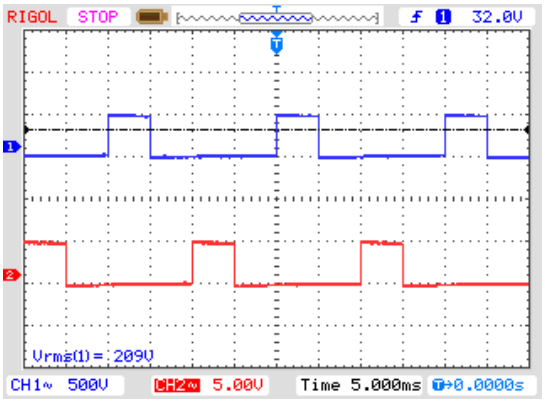

(c) $V_t = 0.975$ pu, $V_{ref} = 1.03$ pu

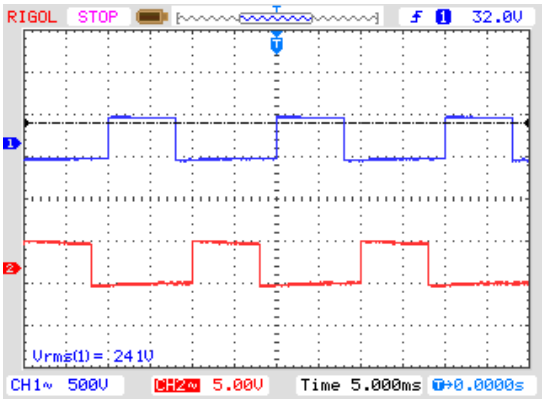

(d) $V_t = 0.975$ pu, $V_{ref} = 1.03$ pu

Figure 9.6: Firing Pulses for T_1 and T_4 for different V_t and V_{ref}

9.2 Response of fully controlled thyristor bridge rectifier

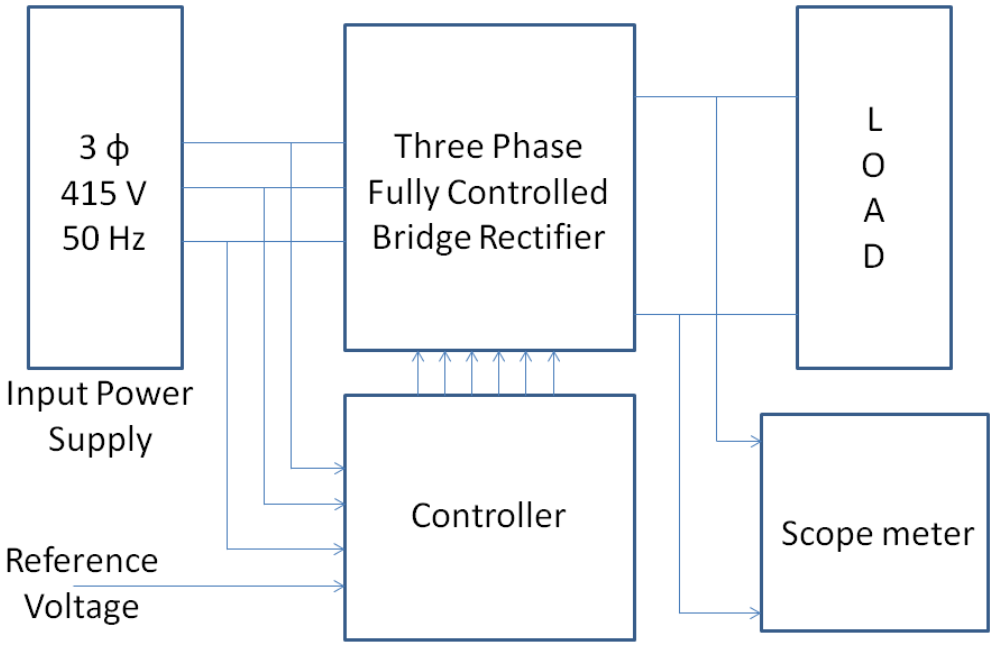

Figure 9.7: Block Diagram of Hardware Implementation

Figure 9.5 shows the block diagram of the hardware implementation where the response of rectifier bridge is observed on scope for a resistive load. Three phase input voltage 415 V, 50 Hz was applied to the rectifier and it is continuously monitored by controller. This voltage can be given from the terminal voltage of the synchronous generator as a feedback through a step down transformer. The reference voltage can be set manually. Hence the controller generates pulses according to the section 9.1. The thyristor provides the response accordingly and are shown in figures 9.6 for different values of voltage V_{dc} which is same as that of the signal E_{fd}. V_{dc} is varied between 5 to 10 V which represents the E_{fd} between 1 to 6 pu. Hence at 10 V we are able to get the field forcing and thus the output voltage is highest. Thus, E_{fd} signal generated irrespective of any algorithm applied, rectifier can accordingly respond thus providing the field voltage to the field winding of the synchronous generator.

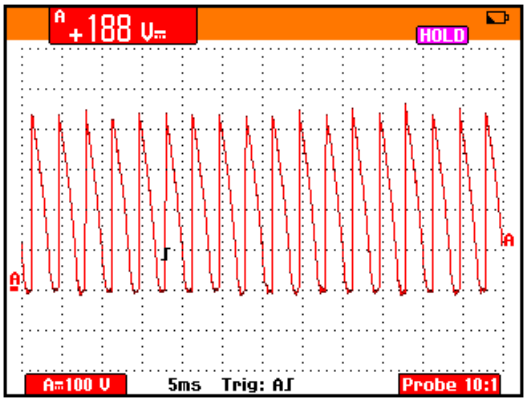

(a) $V_{dc} = 6$ V

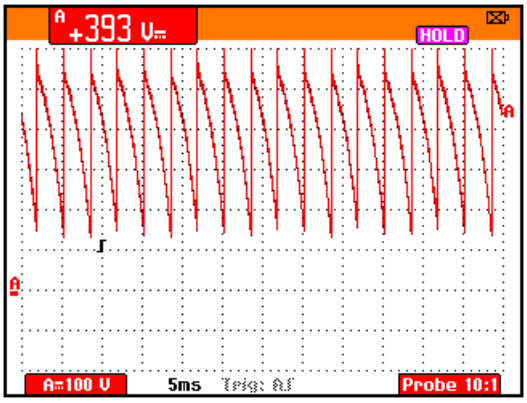

(b) $V_{dc} = 7.5$ V

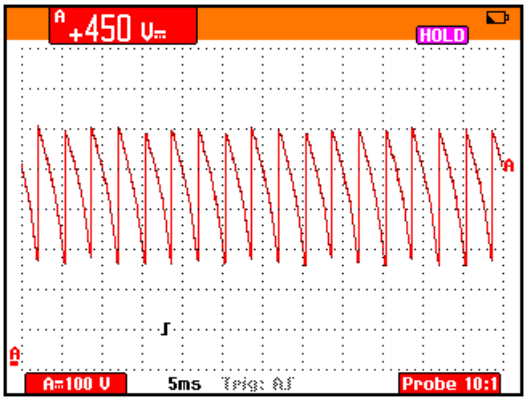

(c) $V_{dc} = 8$ V

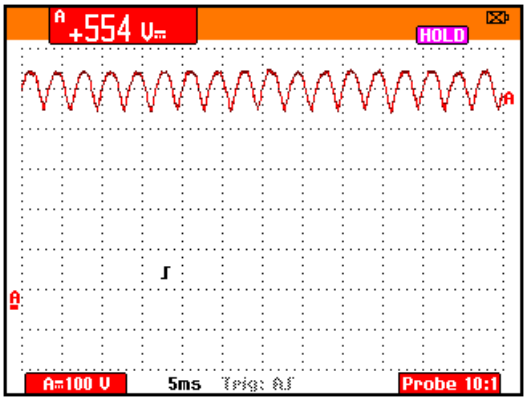

(d) $V_{dc} = 10$ V

Figure 9.8: Thyristor Excitation Response for varying V_{dc}

Chapter 10

Conclusion and Future Scope

10.1 Conclusion

The excitation system response of MATLAB excitation system and Feedback Linearization AVR (FBLAVR) are obtained and compared with each other under both radial system and SMIB system. It is observed that the transient stability of FBLAVR is better. Also the small signal stability obtained is better than conventional AVRs since they provide positive damping torques [2]. The small signal stability is better than conventional [AVR+PSS] for lightly loaded conditions. If the system is weak and it is heavily loaded then [AVR+PSS] provides better performance.
The response of IDA-PBC control is compared with AVR and it is observed that IDA-PBC control provides better small signal stability but since it is not able to provide field forcing transient stability of AVR is better. Thus a combination of both these strategies i.e. AVR+IDAPBC can be implemented. If terminal voltages are within the limits maybe around 2 % then IDA-PBC can be implemented otherwise AVR. In this way transient and voltage stability both can be implemented.
The state estimation of active and reactive powers along with load angle is done. Also the flowchart is provided to obtain the frequency of rotor and active power oscillations.The number of measurements required for the controllers is reduced to four which were generally six to eight. Hence this results in great decrease of overall cost.
Firing pulses were generated on DSpace and thyristor rectifier response was observed. Thus hardware implementation is done.

10.2 Future Scope

New algorithms will be analyzed on SMIB system or IEEE benchmark to obtain better transient, steady and small signal staobility with lower cost, hardware simplicity and better reliability.

Chapter 11

References

1. Francisco P. Demello, Senior Member, IEEE, and Charles Concordia,"Concepts of Synchronous Machine Stability as Affected by Excitation Control,"IEEE Transactions on Power Apparatus and Systems, VOL. PAS-88, NO. 4, APRIL 1969.

2. Gurunath Gurrala and Indraneel Sen,"Synchronizing and Damping Torques Analysis of Nonlinear Voltage Regulators", IEEE Transactions on Power Systems, VOL. 26, NO. 3, August 2011.

3. Gurunath Gurrala, Indraneel Sen, Viswanath Talasila and Purnaprajna Mangsuli, "A Novel Approach for Designing Excitation Controllers Using the IDA-PBC Technique", IEEE, Conference January 2009.

4. IEEE Standard 421

5. A. Godhwani, M.J. Basler, "A Digital Excitation Control System for Use on Brushless Excited Synchonous Generators", IEEE Transactions on Energy Conversion, Vol. 11, No. 3, September1996.

6. P.M. Anderson and A.A. Fouad, "Power System Control and Stability", A. John Wiley and Son, INC., Publication, 2003.

7. Allen J. Wood and Bruce F. Wollenberg, "Power Generation, Operation and Control", John Wiley Sons, 2013.

8. Ramanujam R, "Power System Dynamics: Analysis and Simulation", Prentice Hall of India, Publication, 2009.

9. K R Padhiyar, "Power System Dynamics: Stability and Control", BS Publications, Publication, 2008.

10. Romeo Ortega, Martha Galaz, Alessandro Astolfi, Yuanzhang Sun, and Tielong Shen,"Transient Stabilization of Multimachine Power Systems with Nontrivial Transfer Conductances,"IEEE Transactions on Automatic Control, VOL.50, NO. 1, pp. 60-75, JANUARY 2005

11. Romeo Ortega, Arjan van der Schaft, Bernhard Maschke, and Gerardo Escobar,"Interconnection and Damping Assignment Passivity Based Control of Port Controlled Hamiltonian Systems,"Automatica 38, 585-596, 2002